AD_____

Award Number: W81XWH-18-1-0598

TITLE: Adult-Born Neurons and the Development of Posttraumatic Epilepsy

PRINCIPAL INVESTIGATOR: Eric Schnell

CONTRACTING ORGANIZATION: OREGON HEALTH & SCIENCE UNIVERSITY
PORTLAND OR 97239-3011

REPORT DATE: Sept 2019

TYPE OF REPORT: Annual

PREPARED FOR: U.S. Army Medical Research and Materiel Command
Fort Detrick, Maryland 21702-5012

DISTRIBUTION STATEMENT: Approved for Public Release;
Distribution Unlimited

REPORT DOCUMENTATION PAGE

Form Approved
OMB No. 0704-0188

1. REPORT DATE	2. REPORT TYPE	3. DATES COVERED
Sept 2019	Annual	1 Sep 2018 - 31 Aug 2019

4. TITLE AND SUBTITLE

Adult-Born Neurons and the Development of Posttraumatic Epilepsy

5a. CONTRACT NUMBER

5b. GRANT NUMBER
W81XWH-18-1-0598

5c. PROGRAM ELEMENT NUMBER

6. AUTHOR(S)

Eric Schnell

E-Mail: schneler@ohsu.edu

5d. PROJECT NUMBER

5e. TASK NUMBER

5f. WORK UNIT NUMBER

7. PERFORMING ORGANIZATION NAME(S) AND ADDRESS(ES)

OREGON HEALTH & SCIENCE UNIVERSITY
3181 SW SAM JACKSON PARK RD
PORTLAND OR 97239-3011

8. PERFORMING ORGANIZATION REPORT NUMBER

9. SPONSORING / MONITORING AGENCY NAME(S) AND ADDRESS(ES)
U.S. Army Medical Research and Materiel Command
Fort Detrick, Maryland 21702-5012

10. SPONSOR/MONITOR'S ACRONYM(S)

11. SPONSOR/MONITOR'S REPORT NUMBER(S)

12. DISTRIBUTION / AVAILABILITY STATEMENT
Approved for Public Release; Distribution Unlimited

13. SUPPLEMENTARY NOTES

14. ABSTRACT

Post-traumatic epilepsy (PTE) occurs in over 50% of veterans with a history of penetrating head injury, and individuals with severe head injuries have a seventeen-fold increased risk of developing epilepsy later in life. Although PTE is a heterogeneous condition with multiple etiologies, clinical data suggest that it often involves seizure foci in the temporal lobe, and in particular from within the hippocampus. The hippocampus manifests numerous anatomical changes in epilepsy, which are thought to mediate its contribution to neuronal hyperexcitability and seizures. Although the neuroanatomical changes associated with epilepsy are well described, how these abnormalities lead to the development of epilepsy are unknown. This CDMRP project is analyzing whether newly generated neurons in the hippocampus contribute to the formation of hyperexcitable circuits in a mouse model of posttraumatic epilepsy (PTE). The project's specific aims are (1) to assess adult-born hippocampal granule cell contributions to the formation of recurrent excitatory brain circuits after traumatic brain injury (TBI); (2) to characterize network properties of circuits involving adult-born granule cells after TBI; and (3) to assess whether modulation of posttraumatic neurogenesis by diazepam prevents hippocampal hyperexcitability and posttraumatic epilepsy. If successful, we will not only substantially increase our understanding of how hippocampal function has changed after TBI, but we will also investigate the potential of pharmacologic modulation of the re-wiring process to reduce the subsequent development of epilepsy. This would have great translational relevance to future human clinical trials, which is a major focus of our work.

15. SUBJECT TERMS

Traumatic Brain Injury, Epileptogenesis, Hippocampus, Diazepam, Post-traumatic Epilepsy

16. SECURITY CLASSIFICATION OF:			17. LIMITATION OF ABSTRACT	18. NUMBER OF PAGES	19a. NAME OF RESPONSIBLE PERSON
a. REPORT	b. ABSTRACT	c. THIS PAGE			USAMRMC
U	U	U	UU	32	19b. TELEPHONE NUMBER *(include area code)*

Table of Contents

1. INTRODUCTION

Post-traumatic epilepsy (PTE) occurs in over 50% of veterans with a history of penetrating head injury, and individuals with severe head injuries have a seventeen-fold increased risk of developing epilepsy later in life. Although PTE is a heterogeneous condition with multiple etiologies, clinical data suggest that it often involves seizure foci in the temporal lobe, and in particular from within the hippocampus. The hippocampus manifests numerous anatomical changes in epilepsy, which are thought to mediate its contribution to neuronal hyperexcitability and seizures. Although the neuroanatomical changes associated with epilepsy are well described, how these abnormalities lead to the development of epilepsy are unknown. This CDMRP project is analyzing whether newly generated neurons in the hippocampus contribute to the formation of hyperexcitable circuits in a mouse model of posttraumatic epilepsy (PTE). The project's specific aims are (1) to assess adult-born hippocampal granule cell contributions to the formation of recurrent excitatory brain circuits after traumatic brain injury (TBI); (2) to characterize network properties of circuits involving adult-born granule cells after TBI; and (3) to assess whether modulation of posttraumatic neurogenesis by diazepam prevents hippocampal hyperexcitability and posttraumatic epilepsy. If successful, we will not only substantially increase our understanding of how hippocampal function has changed after TBI, but we will also investigate the potential of pharmacologic modulation of the re-wiring process to reduce the subsequent development of epilepsy. This would have great translational relevance to future human clinical trials, which is a major focus of our work.

2. KEYWORDS

Traumatic Brain Injury, Epileptogenesis, Hippocampus, Diazepam, Post-traumatic Epilepsy

3. ACCOMPLISHMENTS

What were the major goals of the project?

The goal of this proposal is to identify how epilepsy develops after traumatic brain injury, and to identify a strategy to prevent PTE. The development of epilepsy after head injury is often delayed by months or years, which suggests that neuronal circuit functions change slowly over time. Recent work suggests that newly-born hippocampal neurons contribute to hippocmpal circuit changes after TBI, so our hypotheses were that (1) newly born neurons contributed to circuit changes after TBI, (2) that these changes contributed to circuit changes after TBI, and (3) that we could modulate neurogenesis after TBI and reduce circuit rewiring and post-traumatic epilepsy. We are investigating these hypotheses using the following specific aims:

Aim 1: Assess adult-born hippocampal granule cell contributions to the formation of recurrent excitatory brain circuits after TBI. Milestone: Identification of functionally aberrant neuronal inputs and outputs formed by adult-born cells after TBI. Anticipated completion: 14 months. Percent complete: 40%

Aim 2: Assess adult-born granule cell contribution to hippocampal hyperexcitability after TBI. Milestone: Identification and characterization of circuits formed by neurons born

during post-traumatic neurogenesis**.** Anticipated completion: 30 months. Percent complete: 10%

Aim 3: Assess whether modulation of post-traumatic neurogenesis by diazepam prevents hippocampal hyperexcitability and post-traumatic epilepsy (PTE). Milestone 1: Identification of a method to normalize neurogenesis after TBI**.** Anticipated completion: 36 months. Percent complete: 80%**.** Milestone 2: Understanding the role of aberrantly developed adult-born neurons in the pathogenesis of epilepsy, and pre-clinical investigation of a strategy to prevent PTE**.** Anticipated completion: 36 months. Percent complete: 5%.

What was accomplished under these goals?

Major activities: The primary activities in the first year of this proposal quarter involved analysis of circuit rewiring by adult-born hippocampal neurons after TBI. We trained new staff in single cell electrophysiology on acutely prepared mouse brain slices and immunohistochemical techniques, built a new electrophysiology recording setup to be dedicated entirely to this project, and acquired/built a new EEG recording room for the translational analysis of mice after TBI. Finally, we prepared and published a manuscript on the effects of diazepam on post-TBI neurogenesis.

Specific objectives: Throughout this year, we worked to obtain data on the circuit integration of neurons born after injury, and completed a detailed analysis of a potential therapeutic approach to prevent post-traumatic epilepsy. Physiology and imaging experiments are ongoing. We also have maintained a colony of genetically modified mice for analysis, continued to implement regular brain injury modeling, replicated pilot data using our TBI model, and made novel observations.

Significant results: We now also have a large colony of mice for use in these studies, and numerous cohorts of mice undergoing various stages of post-injury recovery. Our new staff have replicated prior results studying the increase in post-traumatic neurogenesis after TBI in our transgenic mouse model. In addition, we completed part of the work on Aim 3 of this proposal, and found that diazepam administration for one week after TBI dramatically reduced the aberrant growth of adult-born neurons born during this phase of post-injury recovery. Finally, our most recent results suggest that loss of a certain hippocampal cell type after TBI may be an integral step in the development of aberrant neurogenesis after TBI, and we are following this line of investigation.

Other Achievements: Our first manuscript directly related to this grant was published in the *Journal of Neurotrauma* on August 15, 2019 (Villasana et al., 2019). For a detailed description of scientific findings, please see this published paper, which is attached in Appendix 1. We also published another paper related to the involvement of hippocampal rewiring in recurrent circuit function, which has significant relevance to the current proposal as it relates to the process of post-seizure neurogenesis (Hendricks et al., 2019, please see Appendix 2).

What opportunities for training and professional development has the project provided?

Although this project was not explicitly intended to provide training and professional development opportunities, two junior scientists obtained significant scientific development through the performance of this work. The contributions of a graduate student (Beeson) and a post-baccalaureate researcher (Wilson) have both had significant training benefits. In the first case, Ms. Beeson obtained experience working with mouse translational models as well as through the mentorship and training of a recently graduated undergraduate, Ms. Wilson. In Ms. Wilson's case, she has been able to learn advanced neuroscience research techniques and obtained insight into future career possibilities.

How were the results disseminated to communities of interest?

Our primary methodology involved publication of manuscripts (see below) for dissemination to the wider scientific community. Additionally, some results from our work on this project have been presented at an international scientific meeting, with the intent of raising awareness amongst perioperative clinicians on the mechanisms of post-injury neurogenesis and how pharmacologic management might modulate this process (Hendricks, W. D., Westbrook, G. L., and Schnell, E. *Sprouted mossy fibers drive epileptiform activity in mice after brain insults*. Association of University Anesthesiologists Annual Meeting; May 16, 2019; Montréal, Canada).

What do you plan to do during the next reporting period to accomplish the goals?

We will continue to maintain our mouse colony and generate mice for the current work. Staff are performing regular TBI modeling experiments, histochemical staining/imaging experiments, and physiologic recordings. Additionally, we have set up a new video-EEG recording rig (4 simultaneous cages; primarily dedicated to this specific project) together with our collaborator Dr. Miranda Lim, and we are beginning to obtain pilot recordings with it. Finally, a new junior faculty member will be joining my lab next spring, and his first project will be to perform video-EEG recordings from mice after TBI and assess how post-traumatic epilepsy is modulated by diazepam. We feel that this aspect of our project has the most translational relevance to the future management of patients with severe head injury, and we have been accelerating preparations to pursue this work.

4. IMPACT

What was the impact on the development of the principal discipline(s) of the project?

Our prior work demonstrated that adult-born hippocampal neurons contributed potently to recurrent circuit formation in epilepsy (*Hendricks, W. D., Chen, Y., Bensen, A.L., Westbrook, G. L., and Schnell, E.; 2017; Short-term Depression of Sprouted Mossy Fiber Synapses from Adult-born Granule Cells. Journal of Neuroscience, 37(23): 5722-5735*), and our more recent work demonstrated that these recurrent circuits potently drive epileptiform activity (Hendricks et al. 2019; see Appendix 2). Together, these data strongly suggest that the aberrant neurogenesis leads to circuit hyperexcitability, and may directly contribute to epileptic seizures.

Through recent experiments performed as part of this proposal, we have discovered that diazepam can potently modulate (and normalize) post-injury neurogenesis. In light of our prior data, we hypothesize that this may have significant implications on the subsequent occurrence of seizures after TBI. If our mouse EEG recordings validate this hypothesis, this could directly impact future clinical research, including the development of clinical

trials and potential therapeutic management approaches after TBI which include short-term administration of diazepam to normalize early post-traumatic neuronal circuit remodeling, with the goal of reducing the incidence of epilepsy after head injury.

What was the impact on other disciplines?

Nothing to Report.

What was the impact on technology transfer?

Nothing to Report.

What was the impact on society beyond science and technology?

Nothing to Report.

5. CHANGES/PROBLEMS

Changes in approach and reasons for change

We have deviated from our expected timeline by accelerating the most translational aim (Aim 3), which is now partly completed well ahead of our original schedule. This was done intentionally, as it will allow us to proceed with our EEG experiments in epileptic mice ahead of schedule as well. Otherwise, we are continuing with our experiments as originally proposed, with the only minor change comprising of the addition of some immunohistochemical experiments to help further characterize some additional morphologic circuit changes that we have noticed after TBI. This is in response to some compelling preliminary data coming from a related project in the lab, suggesting a possible mechanism that could explain the aberrant neurogenesis after TBI. We still plan to perform the originally proposed experiments, but will likely obtain additional data and perhaps be able to refine/improve our approaches accordingly.

Actual or anticipated problems or delays and actions or plans to resolve them

No problems/issues anticipated at this time. As mentioned previously in our quarterly reports, our initial data collection was delayed due to the need to breed and age the appropriate experimental animals (experiments are begun in mice at 2 months of age, and analyzed an additional 2 months later; thus a guaranteed 5 months before the first data were acquired). Additionally, due to local hiring constraints and logistic processes, there was a substantial delay in the on-boarding of a new staff member dedicated to this project despite the PI's best and most aggressive efforts. The PI is always aware of the potential for staff turnover, breeding colony issues, and equipment failure, and thus is constantly working to acquire spare staff and equipment capacity, to prevent these potential issues from negatively impacting experimental progress.

Changes that had a significant impact on expenditures

Due in part to the delayed start to data acquisition, we are currently below budget. However, we expect our overall budget for these experiments to remain the same.

Significant changes in use or care of human subjects, vertebrate animals, biohazards, and/or select agents

Nothing to report.

6. PRODUCTS

One manuscript directly related to the Scope of Work in this proposal was published last month (see Appendix 1):

> Villasana, L. E., Peters, A. J., McCallum, R., Liu, C., and Schnell, E. (2019) Diazepam inhibits post-traumatic neurogenesis and blocks aberrant dendritic development. *Journal of Neurotrauma*, 36: 2454-2467.

In addition, our lab published a second manuscript (described above), that was based in part upon technical developments undertaken in preparation for this proposal, and which we believe has direct relevance to post-traumatic circuit rewiring that we have reported after TBI. We have included this manuscript as Appendix 2, as it has helped guide our work on this CDMRP proposal, and is evidence of the synergy that is possible when combining multiple translational models in a single lab.

> Hendricks, W. D., Westbrook, G. L., and Schnell, E. (2019) Early detonation by sprouted mossy fibers enables aberrant dentate network activity. *Proceedings of the National Academy of Sciences, U.S.A.,* 116(22):10994-10999.

Indirectly related to this project, we have generated additional manuscripts that investigate the fundamental mechanisms underlying the control of circuit plasticity and/or development of epilepsy, as it relates to the neurogenic niche in the hippocampal dentate gyrus. The citations for these works are noted here for your reference:

> Gupta, K. and Schnell, E. (2019) Post-ictal neuronal network remodeling and Wnt pathway dysregulation in the intra-hippocampal kainate mouse model of temporal lobe epilepsy. *bioRxiv*, 10.1101/604975. [Preprint]

> Beeson, K. A., Beeson, R., Westbrook, G. L., and Schnell, E. (2019) α2δ-2 protein controls structure and function at the cerebellar climbing fiber synapse. *bioRxiv*, 10.1101/604975. [Preprint]

> Chatzi, C., Zhang, Y., Hendricks, W. D., Chen, Y., Schnell, E., Goodman, R. H. and Westbrook, G. L. (2019) Exercise-induced enhancement of synaptic function triggered by the inverse BAR protein, Mtss1L. *eLife* 8:e45920.

Data from this project also contributed to a presentation at an international scientific meeting, as mentioned above:

> Hendricks, W. D., Westbrook, G. L., and Schnell, E. *Sprouted mossy fibers drive epileptiform activity in mice after brain insults*. Association of University Anesthesiologists Annual Meeting; May 16, 2019; Montréal, Canada

7. PARTICIPANTS

Name: *Eric Schnell*
Project Role: *Principal Investigator*
Researcher Identifier (ORCID ID): 0000-0002-5623-5015
Nearest person month worked: *3*
Contribution to Project: *Dr. Schnell initiated the project, prepared preliminary data and proposal, hired staff, trained staff, analyzed preliminary data.*
Funding Support: *Dept of Veterans' Affairs*

Name: *Laura Villasana*
Project Role: *Collaborator*
Researcher Identifier (eRA Commons): VILLASAN
Nearest person month worked: *3*
Contribution to Project: *Dr. Villasana produced preliminary data for the project, is co-authoring a manuscript with the PI on work related to this proposal, and is training new staff in procedures*
Funding Support: *OHSU Department of Anesthesiology*

Name: *Miranda Lim*
Project Role: *Collaborator*
Researcher Identifier (eRA Commons): 100010401
Nearest person month worked: *2*
Contribution to Project: *Dr. Lim is a collaborator that will be assisting with EEG recordings from mice with post-traumatic epilepsy; in this past year she assembled a new 4-cage EEG recording apparatus (purchased by Dr. Schnell specifically for this CDMRP project) and has been testing it with validation cohorts so that it is fully operational for next years' recordings.*
Funding Support: *Dept of Veterans' Affairs*

Name: *Kathleen Beeson*
Project Role: *Graduate Student*
Researcher Identifier (eRA Commons): *KBEESON*
Nearest person month worked: *6*
Contribution to Project: *Ms. Beeson continues to train and oversee staff in the procedures necessary for this project*
Funding Support: *OHSU Department of Anesthesiology*

Name: *Alexandria Wilson*
Project Role: *Research Assistant*
Researcher Identifier: n/a
Nearest person month worked: *8*
Contribution to Project: *Ms. Wilson was specifically hired to work on this project, has been breeding mice, performing TBI models in mice, staining/analyzing post-TBI tissue, and performing electrophysiologic recordings for this project.*
Funding Support: *Dept of Veterans' Affairs*

Changes in active other support of the PD/PI(s) or senior/key personnel since the last reporting period:

Nothing to report.

Changes in other organizations involved as partners:

Nothing to report.

8. SPECIAL REPORTING REQUIREMENTS

Quad chart provided on next page.

Adult-Born Neurons and the Development of Posttraumatic Epilepsy

USAMRMC Proposal Number EP170012
W81XWH-18-1-0598

PI: Eric Schnell **Org:** Oregon Health and Science University **Award Amount:** $500,000

Study/Product Aim(s)

- Assess adult-born hippocampal granule cell contributions to the formation of recurrent excitatory brain circuits after TBI
- Assess adult-born granule cell contribution to hippocampal hyperexcitability after TBI
- Assess whether modulation of post-traumatic neurogenesis by diazepam prevents hippocampal hyperexcitability and post-traumatic epilepsy

Approach

We are using a model of post-TBI epilepsy in a new line of genetically modified mice to investigate the neurobiology that causes epilepsy after head injury. We are imaging brain tissue, performing electrical recordings of brain circuit function, and performing mouse EEG recordings to characterize how seizures occur and to evaluate a treatment strategy to prevent epilepsy after TBI.

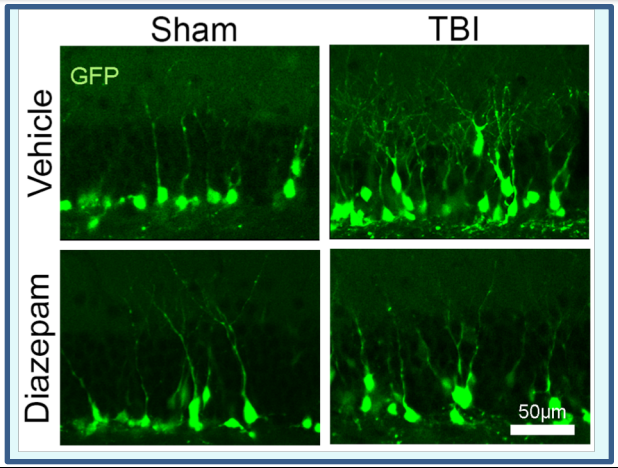

Accomplishment: Using a transgenic mouse in which adult-born neurons are filled with a green fluorescent protein, we found that diazepam administration for one week after traumatic brain injury (TBI) prevents aberrant neurogenesis (as published in Villasana et al. 2019; *J Neurotrauma, 36:2454*).

Timeline and Cost

Activities CY	18	19	20	21
Identify circuit changes after TBI				
Identify how hyperexcitability occurs				
Strategy to prevent circuit changes				
Strategy to prevent post-TBI epilepsy				
Estimated Budget ($K)	**$ 56**	**$167**	**$167**	**$111**

Updated: 9/15/2019

Goals/Milestones

CY18 Goal – Develop research model and hire staff
☑ Staff hired and trained, experiments in progress
CY19 Goals – Functional characterization of adult-born neurons
☑ Imaging of tissue (ongoing)
☑ Electrophysiologic recordings (ongoing)
CY20 Goals – Characterize hyperexcitability
☐ Recordings of output circuitry
☐ Establish EEG recordings
CY21 Goal – Test therapeutic strategy
☐ Test effects using EEG recordings from treated mice

Comments/Challenges/Issues/Concerns

- No concerns at this time

Budget Expenditure to Date

Projected Expenditure: $167K
Actual Expenditure: ~$117K

9. APPENDICES

Please see the attached manuscripts (Appendix 1 – Villasana et al.; Appendix 2 – Hendricks et al.).

JOURNAL OF NEUROTRAUMA 36:2454–2467 (August 15, 2019)

DOI: 10.1089/neu.2018.6162

Diazepam Inhibits Post-Traumatic Neurogenesis and Blocks Aberrant Dendritic Development

Laura E. Villasana,[1] Austin Peters,[1] Raluca McCallum,[2] Chang Liu,[1] and Eric Schnell[1,2]

Abstract

Traumatic brain injury (TBI) triggers a robust increase in neurogenesis within the dentate gyrus of the hippocampus, but these new neurons undergo aberrant maturation and dendritic outgrowth. Because gamma-aminobutyric acid $(GABA)_A$ receptors ($GABA_A$Rs) modulate dendritic outgrowth during constitutive neurogenesis and $GABA_A$R-modulating sedatives are often administered to human patients after TBI, we investigated whether the benzodiazepine, diazepam (DZP), alters post-injury hippocampal neurogenesis. We used a controlled cortical impact (CCI) model of TBI in adult mice, and administered DZP or vehicle continuously for 1 week after injury via osmotic pump. Although DZP did not affect the neurogenesis rate in control mice, it almost completely prevented the TBI-induced increase in hippocampal neurogenesis as well as the aberrant dendritic growth of neurons born after TBI. DZP did not reduce cortical injury, reactive gliosis, or cell proliferation early after injury, but decreased c-Fos activation in the dentate gyrus at both early and late time-points after TBI, suggesting an association between neuronal activity and post-injury neurogenesis. Because DZP blocks post-injury neurogenesis, further studies are warranted to assess whether benzodiazepines alter cognitive recovery or the development of complications after TBI.

Keywords: controlled cortical impact; diazepam; models of injury; neurogenesis; regeneration; traumatic brain injury

Introduction

In 2010, approximately 2.5 million people in the United States sustained a traumatic brain injury (TBI), and over the past decade, the rate of TBI has increased in men and women by 63% and 49%, respectively.[1] As the rate of TBI-related death has declined, more people now live with TBI-related cognitive and emotional impairments.[1–5] It was long believed that recovery from TBI was in part limited by the irreversible loss of neurons; however, we now know that the adult brain has a limited capacity for self-renewal through the process of adult neurogenesis.[6,7] In the hippocampus, adult-born dentate granule cell neurons are important for learning and memory,[8–10] and may also play important roles in emotional regulation.[11,12]

TBI robustly increases hippocampal neurogenesis,[13–18] and augmentation of this process after TBI could facilitate cognitive recovery.[19–22] Alternatively, as neurons born after various neuronal injuries have functional and morphological abnormalities,[23–27] they could drive negative outcomes such as the development of post-traumatic epilepsy.[28–30] Either way, the net effect of post-TBI neurogenesis on recovery likely depends on the maturation and neuronal circuit integration of the neurons born after injury.

A variety of signaling mechanisms modulate adult hippocampal neurogenesis, including ionotropic neurotransmitter receptors.[31–33] Specifically, gamma-aminobutyric acid type A receptors ($GABA_A$Rs) modulate the proliferation of neuronal stem cells and neuronal maturation.[33–36] $GABA_A$Rs are also the targets of sedative and anesthetic drugs[37] including benzodiazepines and propofol, which are often administered to hospitalized patients after severe head injury,[38] and thus could affect cell proliferation, maturation, and survival both during constitutive and post-injury adult neurogenesis.[39–41]

Thus, we asked whether the prototypical benzodiazepine, diazepam (DZP), administered after TBI affects post-traumatic neurogenesis. We used a controlled cortical impact (CCI) model of TBI in wild-type and in transgenic *POMC-GFP* mice, in which green fluorescent protein (GFP) is selectively expressed by immature adult-born hippocampal neurons. DZP was administered continuously by osmotic pump for 7 days, beginning shortly after CCI or sham injury. We subsequently analyzed hippocampal neurogenesis and histopathological markers in injured and control brains to determine whether DZP modulates post-traumatic neurogenesis.

Methods

Animals

All procedures were performed in accordance with the National Institutes of Health Guide for the Care and Use of Laboratory

[1]Department of Anesthesiology and Perioperative Medicine, Oregon Health & Science University, Portland, Oregon.
[2]Operative Care Division, VA Portland Health Care System, Portland, Oregon.

Animals and were approved by the Institutional Animal Care and Use Committee at Oregon Health & Science University (OHSU). Male and female C57Bl/6J wild-type mice were obtained from Jackson Labs, and heterozygotic *POMC-GFP* mice[42] were obtained by crossing homozygotic mice (maintained on a C57 background) with wild-type mice.

Controlled cortical impact injury and diazepam administration

We used a CCI model of TBI in 2-month-old mice as previously described.[23,43] Briefly, mice were placed under isoflurane anesthesia (2% spontaneously inhaled) and mounted on a stereotaxic frame. After sterile skin preparation and a midline scalp incision, a 4-mm craniotomy was made unilaterally bordering right of the midline between lambda and bregma, keeping dura intact. TBI was induced with a 0.9-mm deformation (4.4 m/sec; 800 msec dwell) delivered directly onto the exposed dura using an electromagnetic impactor with a 3-mm cylindrical tip (ImpactOne, Leica Microsystems). Sham mice underwent the same surgery and anesthesia minus the craniotomy and impact.

After CCI or sham treatment, the scalp was closed using sutures and Vetbond adhesive. While still anesthetized, each mouse was subcutaneously implanted with a mini-osmotic pump (AlzetAP2001; Cupertino, CA) containing either vehicle (1:1 dimethyl sulfoxide [DMSO]:propylene glycol) or DZP (added to vehicle for a dose of 15 mg/kg/day), and which had been pre-equilibrated in saline per the manufacturer's instructions. Mice were given ear punches for identification and allowed to recover in a warm padded chamber for 1 h. Osmotic pumps delivered solutions at a rate of 1 μL/h for 1 week and were then surgically removed under isoflurane anesthesia. Residual volumes in the pump were all ±10% of predicted volumes based on the implantation/equilibration time. *POMC-GFP* mice were sacrificed 2 weeks after sham/CCI for histological analysis. For any group, littermates were divided between sham and CCI treatment and between vehicle and DZP pump implantation.

The number of *POMC-GFP* mice for each group was: 10 sham-vehicle (7 females, 3 males), 9 CCI-vehicle (5 females, 4 males), 7 sham-DZP (3 females, 4 males), and 11 CCI-DZP (5 females, 6 males). The number of wild-type mice assessed 3 weeks after CCI (for BrdU labeling, DCX expression) was 6 sham-vehicle (3 females, 3 males), 7 CCI-vehicle (3 females, 4 males), 7 sham-DZP (4 females, 3 males), and 6 CCI-DZP (3 females, 3 males). The number of wild-type mice assessed 3 days after CCI included a total of 12 sham-vehicle (7 females, 5 males), 13 CCI-vehicle (8 females, 5 males), 14 sham-DZP (10 females; 4 males), and 13 CCI-vehicle (9 females, 4 males). A third cohort of 16 wild-type male mice was sacrificed 3 h after sham or CCI treatment with pump implantation, and used to determine the acute effects of DZP on neuronal activity and cell death. The number of mice per group is reported in the legend of the figure for each outcome.

BrdU protocol

Wild-type mice received two intraperitoneal injections (4 h apart) of the mitotic marker bromodeoxyuridine (BrdU, 300 mg/kg dissolved in saline) daily for 2 days, beginning 2 days after CCI or sham. This saturating BrdU dose provides long-term labeling of dividing cells and their progeny.[44] These mice were sacrificed at 3 weeks to assess the density of $BrdU^+$ cells. Neuronal fate specification of $BrdU^+$ cells was assessed using co-labeling with the neuronal marker doublecortin (DCX). To determine the effects of DZP on cell proliferation within the dentate gyrus, a separate cohort of wild-type mice was injected with BrdU (50 mg/kg) every 2 h for 6 h on the second day after surgery, and then sacrificed the following day to minimize the effects of differential early survival on the $BrdU^+$ cell count.[45] This lower dose was chosen to provide a continuous level of BrdU for an extended period during the labeling day, without the need to label multiple rounds of cell division given the shorter experimental time frame. We did not observe any sex differences in regard to post-traumatic neurogenesis or cell proliferation in any of our assays, and thus results for both sexes were combined.

Immunohistochemistry

Immunohistochemistry was performed as previously described[23] with some modifications. Following a terminal dose of avertin (1.2%, 1 mL, intraperitoneal [i.p.]), mice were transcardially perfused with phosphate-buffered saline (PBS) followed by 4% paraformaldehyde in PBS. Brains were harvested and post-fixed overnight. Free-floating coronal sections (150 μm thick) were then prepared using a vibratome. Four sections containing the hippocampus (two dorsal: approximately −1.46 and −2.18 mm from bregma; and two ventral: approximately −2.54 and −2.80 mm from bregma) from each mouse were permeabilized in 0.4% Triton in PBS (PBST) for 45 min and then blocked for 30 min with 10% horse serum (HS) in PBST. The sections were then incubated overnight (4°C) with primary antibodies diluted in PBST with 1.5% HS. These included rabbit anti-GFP (Alexa Fluor 488 conjugated; 1:400, Invitrogen), goat anti-doublecortin (1:400, Santa Cruz), rat anti-BrdU (1:400, Abcam), rabbit anti-c-Fos (1:400, Santa Cruz), rat anti-Ki67 (1:400, eBioscience), and rabbit anti-GFAP (1:1000, DAKO). Sections stained with anti-BrdU were first denatured in 2N hydrochloric acid in potassium-PBS for 30 min (37°C) followed by a neutralization step (potassium-PBS pH 8.5) prior to staining.

After primary antibody incubation, sections were washed in PBST and exposed to fluorophore-conjugated secondary antibodies (Invitrogen) dissolved in PBST +1.5% HS for 4 h at room temperature. The sections were then washed in PBST containing DAPI (1:20,000) and mounted on slides with Fluoromount-G (Southern Biotech).

Cell death was assessed 3 days after surgery using Fluoro-Jade C (Histo-chem) staining following the manufacturer's protocol. Slices were mounted on gelatinized slides and allowed to air dry at room temperature before immersion in 100% ethanol (3 min), 70% ethanol (1 min), and deionized water (1 min). The slides were then immersed and gently shaken in 0.06% potassium permanganate for 15 min followed by 0.001% Fluoro-Jade C for 30 min. The slides were washed in water for 1 min 3 times before they were allowed to dry overnight. The next day, the slides were dipped in xylene 3 times (2 min each time) and cover-slipped with DPX (Electron Microscopy Sciences, Inc.). In a separate cohort of animals, cell death in the granule cell layer (GCL) and surrounding tissue was assessed in mice sacrificed 3 h after injury (using the same staining protocol), to determine whether DZP exerted an immediate effect on cell death after CCI.

Confocal microscopy and image analysis

Slides were coded, and the hippocampus of each mouse was imaged with a Zeiss LSM780 confocal microscope using a 10×0.45 NA or 20×0.8 NA lens, by an experimenter blinded to experimental condition. All subsequent analyses were performed on coded images with ImageJ software.

In BrdU-stained slices from wild-type mice taken either 3 days or 3 weeks after CCI, all DCX/BrdU double positive cells were counted throughout a 50-μm image stack of the dentate GCL and the subgranular zone (SGZ), and normalized to the GCL volume. GCL volume was obtained by multiplying the cross-sectional area of the GCL in the first optical section by the depth of image stack. Quantification of Ki-67 staining from mice 3 days after CCI was performed similar to the BrdU quantification, but sections were imaged and counted using a 25-μm image stack of dentate GCL and SGZ. To determine the effects of DZP and CCI on neuronal

activity, slices were stained for the activity-dependent gene c-Fos at early and late time-points during treatment. In the mice assessed 3 days after CCI, cells within the dentate gyrus positive for c-Fos were counted in a 30-μm thick z-stack of the GCL. In a separate cohort of mice assessed 3 h after CCI, due to the high density of c-Fos$^+$ cells within the dentate gyrus GCL, the mean intensity of all pixels corresponding to the GCL (determined via DAPI signal) within a single confocal section was used to compare group differences. Intensity values were normalized by dividing the mean pixel intensity for each image by the mean c-Fos pixel intensity from the sham/vehicle stained slices (which was set to 100%).

To compare glial fibrilary acidic protein (GFAP) staining between groups, the mean pixel intensity in images of the dentate hilus and the molecular layer was obtained with ImageJ, and all values were normalized to the mean GFAP pixel intensity from the sham/vehicle stained slices. To count Fluoro-Jade C$^+$ cells, single confocal sections of the dentate gyrus from multiple slices (minimum of 3) bracketing the injury cavity were used for each mouse. The somatosensory cortex was also analyzed separately to assess Fluoro-Jade C$^+$ cell counts and staining quality at the 3 h time-point. For all imaging experiments, samples were identically processed (side-by-side), imaging parameters were kept constant between slides, and blinded investigators performed imaging and image analysis.

To quantify post-traumatic neurogenesis in *POMC-GFP* mice, the ipsilateral hippocampus was imaged from tissue harvested 2 weeks after sham or CCI. This time-point was chosen to allow analysis of the same population of cells labeled by BrdU in wild-type mice, as GFP is expressed by immature, adult-born neurons between 10 and 14 days post-mitosis.[42] GFP$^+$ cells were counted on single confocal sections from 2 to 4 slices per mouse that included the molecular layer, the GCL, and theSGZ of the dentate gyrus. The cell count was normalized to the imaged GCL area of each slice to estimate GFP$^+$ cell density.

The cortical cavity in mice that underwent CCI treatment was assessed 3 days after surgery by subtracting the area of the ipsilateral cortex immediately beneath the impact site (using a tiled image acquired with overlapping 4$\times$ images) from the area of the contralateral cortex from the same slice. All anatomical measurements were collected and analyzed by an investigator blinded to the group assignment of each animal.

Cell migration and morphology

As adult-born neurons mature, they slowly migrate from the SGZ of the dentate gyrus outward into the GCL. To determine whether DZP influences cell migration, the linear distance from the center of each cell body to the SGZ/hilar border was measured in the confocal image plane traversing mid-nucleus, using ImageJ as previously described.[23] Cells that migrated backward into the hilus or out into the molecular layer (defined as migration >10 μm away from the inner border of the SGZ or the outer border of the GCL, respectively) were counted separately to quantify ectopically migrated cells. Ectopically migrated cells were quantified using single confocal sections of the dentate gyrus.

To quantify dendritic morphology, we traced the morphology of GFP$^+$ cells from confocal stack images using ImageJ as previously described.[23] GFP$^+$ cell dendritic trees were imaged in their entirety (three dimensions) using a confocal stack, and traced in ImageJ. An average of 5 to 8 cells were traced for 3 to 4 mice/group, and these cell tracings were analyzed using the ImageJ Sholl analysis plug-in (Ghosh Lab, http://labs.biology.ucsd.edu/ghosh/software/). All analyses were performed by an experimenter blinded to experimental condition.

Open field analysis following CCI and during diazepam administration

The open field test was used to assess locomotor and exploratory behavior to determine whether the dose of DZP administered had any gross effects on mouse activity levels. Three days following sham or CCI treatment (during DZP or vehicle delivery), mice were acclimated to single housing for 1 h in a holding room during the morning hours. After acclimatization, they were individually introduced to an open field (40-cm$\times$40-cm white chamber; 200 lux luminescence) for 10 min each. The distance traveled, rearing events (postured upright on rear legs), and velocity were assessed using video recording and tracking software (Noldus, Ethovision).

Experimental design and statistical analysis

Sample sizes were determined for each group through power analyses using estimates of effect magnitude and variability to detect significance at $p<0.05$ with a power of 80%. For all statistical analyses, data normality was first assessed to determine use of parametric or non-parametric tests as indicated in the Results section. For parametric statistics, a two-way ANCOVA (analysis of co-variance) was used to compare group differences and potential interactions. The between-subjects variables consisted of CCI treatment, DZP exposure, and sex, and litter was used as a covariate to account for potential variability in cell labeling densities between litters. A repeated measures analysis of variance (ANOVA) was used to compare group differences in the Sholl analysis with the distance from the soma as the within-subject factor and CCI and DZP treatment as the between-subject factors. A Bonferroni post hoc test was used to compare specific distance points when there was a significant interaction between the variables. For non-parametric statistics, a Mann-Whitney test was used to compare CCI-treated groups with their respective vehicle or DZP controls. All figures and statistical analyses were conducted using Prism (GraphPad Software, La Jolla, CA) and SPSS (IBM SPSS, Armonk, NY) software. Data are expressed as mean$\pm$standard error of the mean (SEM) and comparisons were considered significant at $p<0.05$. The number of mice for each time-point and analysis are noted in the Methods section and figure legends.

Results

Diazepam inhibits post-traumatic neurogenesis

To determine the effect of DZP on post-traumatic neurogenesis, wild-type mice were implanted with osmotic pumps after CCI or sham procedures, to deliver DZP (or vehicle) continuously for 7 days at a sub-anesthetic dose of 15 mg/kg/day (Fig. 1A). This dose was chosen for its demonstrated pre-clinical efficacy,[46] and continuous delivery was used to model prolonged sedative exposure as well as to account for the short serum half-life of DZP in rodents (54–66 min).[47,48] These mice were injected with the mitotic marker BrdU on post-procedure days 2 and 3, to coincide with the peak level of post-traumatic neurogenesis,[13,18] and analyzed 3 weeks later using immunohistochemistry.

Consistent with prior reports,[49] CCI increased hippocampal neurogenesis (BrdU$^+$/DCX$^+$ cell density; see Methods section) in vehicle-treated mice (sham-vehicle vs. CCI-vehicle; $p=0.001$, Mann-Whitney test; Fig. 1B,C). However, DZP treatment for 1 week after CCI completely prevented the CCI-induced enhancement in neurogenesis (sham-DZP vs. CCI-DZP; $p=0.12$, Mann-Whitney test; Fig. 1B,C). Interestingly, DZP had no effect on neurogenesis rate in sham-treated mice (sham-vehicle vs. sham-DZP; $p=0.81$, Mann-Whitney test; Fig. 1B,C). Thus, a sub-anesthetic dose of DZP prevented post-traumatic neurogenesis without affecting constitutive adult neurogenesis.

As these BrdU$^+$ cells were generated during a 2-day time window early after injury, we broadened our analysis by quantifying overall DCX$^+$ cell density, which would also include cells generated after DZP cessation, based on the known expression pattern of

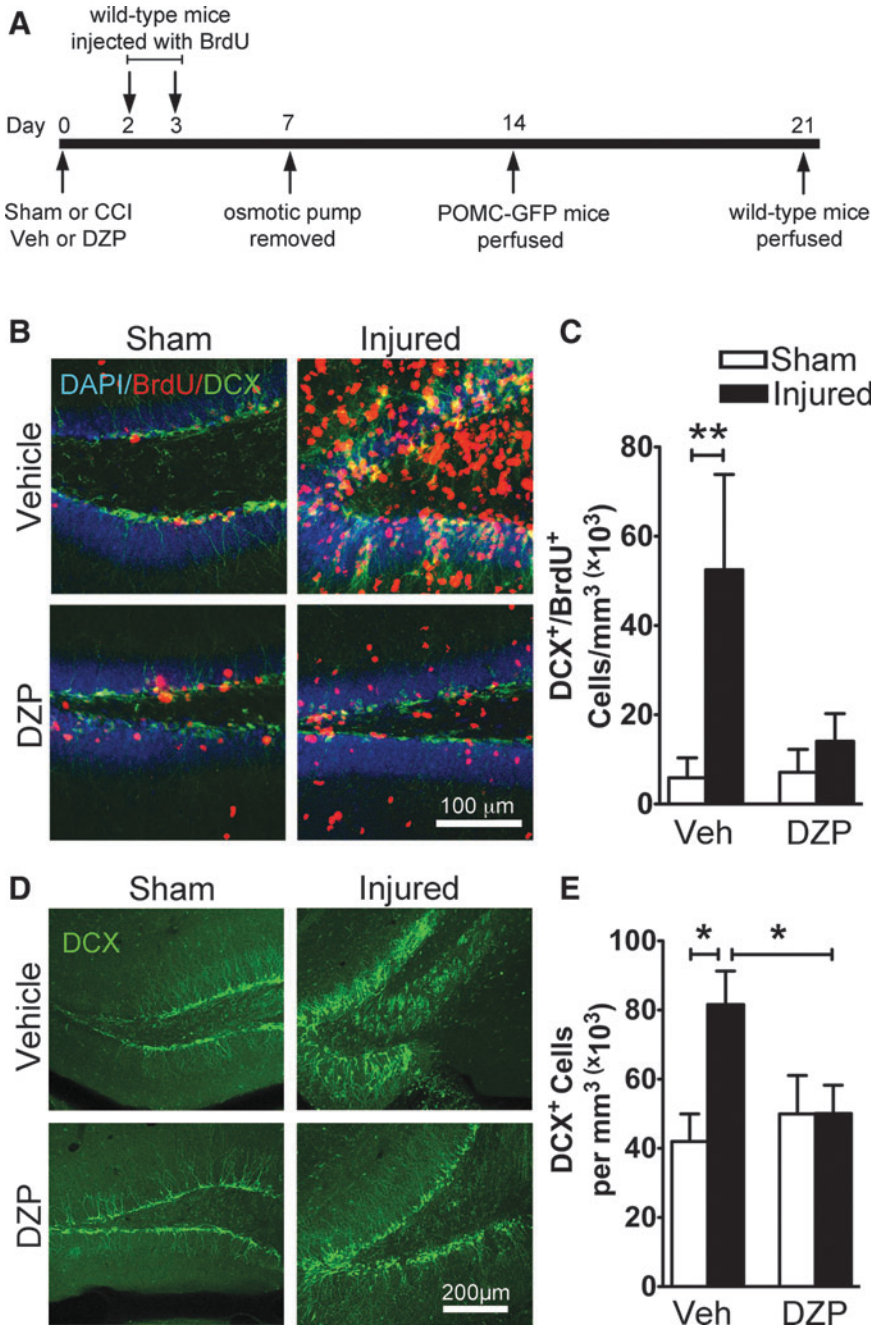

FIG. 1. Diazepam (DZP) inhibits post-traumatic hippocampal neurogenesis. **(A)** Experimental design. Two-month-old male and female *POMC-GFP* and C57Bl/6J wild-type mice underwent a controlled cortical impact (CCI) injury or sham procedure, and were subsequently implanted with osmotic pumps releasing vehicle (Veh) or DZP. On the second and third day after surgery, wild-type mice received two injections of BrdU per day. Osmotic pumps were left in place for 1 week and hippocampal neurogenesis was analyzed 2 or 3 weeks later (separate cohorts). **(B)** Confocal image projections of the dentate gyrus of wild-type mice perfused 3 weeks after injury, co-labeled with the neuronal marker doublecortin (DCX) and the mitotic marker BrdU. BrdU was overexposed (equally in all images) to clearly illustrate all $BrdU^+$ cells, including dim cells, against the green DCX^+ cells. **(C)** Quantification of $BrdU^+/DCX^+$ cell density within the granule cell layer of the dentate gyrus. $BrdU^+/DCX^+$cell density was increased after CCI in vehicle-treated mice; however, this increase was prevented in injured mice that received DZP immediately after injury (**$p < 0.01$, sham-vehicle vs. CCI-vehicle treated mice; $n = 6$–9 mice/group). **(D)** Confocal images of the dentate gyrus of wild-type mice stained for DCX. **(E)** Quantification of DCX^+ cell density within the granule cell layer of the dentate gyrus. CCI increased the density of DCX^+ cells in vehicle-treated but not DZP-treated mice (*$p < 0.05$ CCI-vehicle vs. sham-vehicle and CCI-DZP treated mice, $n = 6$–9 mice/group).

DCX from 1 to 3 weeks post-mitosis.[50] Three weeks after CCI, DCX staining showed a similar pattern (Fig. 1D), as DZP prevented the CCI-induced increase in DCX^+ cell density (drug × CCI interaction $F[1, 23] = 4.970$; $p = 0.036$; two-way ANCOVA; Fig. 1E). CCI increased the density of DCX^+ cells in vehicle-treated mice (main effect of CCI, $F[1,14] = 8.94$; $p = 0.011$; Fig. 1D,E), whereas CCI did not alter the density of DCX^+ cells when followed by 1 week of DZP treatment (CCI-DZP vs. sham-DZP; $p = 0.941$; Fig. 1E). DZP treatment did not affect DCX expression in sham-treated mice (sham-vehicle vs. sham-DZP; $p = 0.430$; Fig. 1E), again indicating that a continuous sub-anesthetic dose of benzodiazepine does not affect constitutive neurogenesis.

Diazepam does not inhibit cell proliferation after TBI

The DZP-mediated inhibition of post-traumatic neurogenesis could result from altered stem cell proliferation after CCI in the presence of DZP, or alternatively via differential survival of neuronal precursors.[51] To directly measure the effect of DZP on cell proliferation during the peak period of post-traumatic neurogenesis, we repeated our CCI protocol on a cohort of mice injected with BrdU on post-surgery day 2, and analyzed hippocampal tissue on post-surgery day 3.[13,18] In vehicle-treated animals, CCI dramatically increased cell proliferation, as assessed by the density of newly post-mitotic cells in the GCL/SGZ ($p = 0.032$; sham-vehicle vs. CCI-vehicle; Mann-Whitney test; Fig. 2A,B). Surprisingly, DZP did not prevent the CCI-induced increase in cell proliferation ($p = 0.030$; sham-DZP vs. CCI-DZP; Mann-Whitney test; Fig. 2A,B), in sharp contrast with the DZP-mediated inhibition of neurogenesis noted at later timepoints (Fig. 1). DZP also did not alter proliferation in sham-treated mice, as assessed by $BrdU^+$ cell density ($p = 0.556$; sham-vehicle vs. sham-DZP; Mann-Whitney test; Fig. 2A,B).

To further investigate this observation with an independent assay, we stained hippocampal tissue for Ki67, a nuclear antigen that

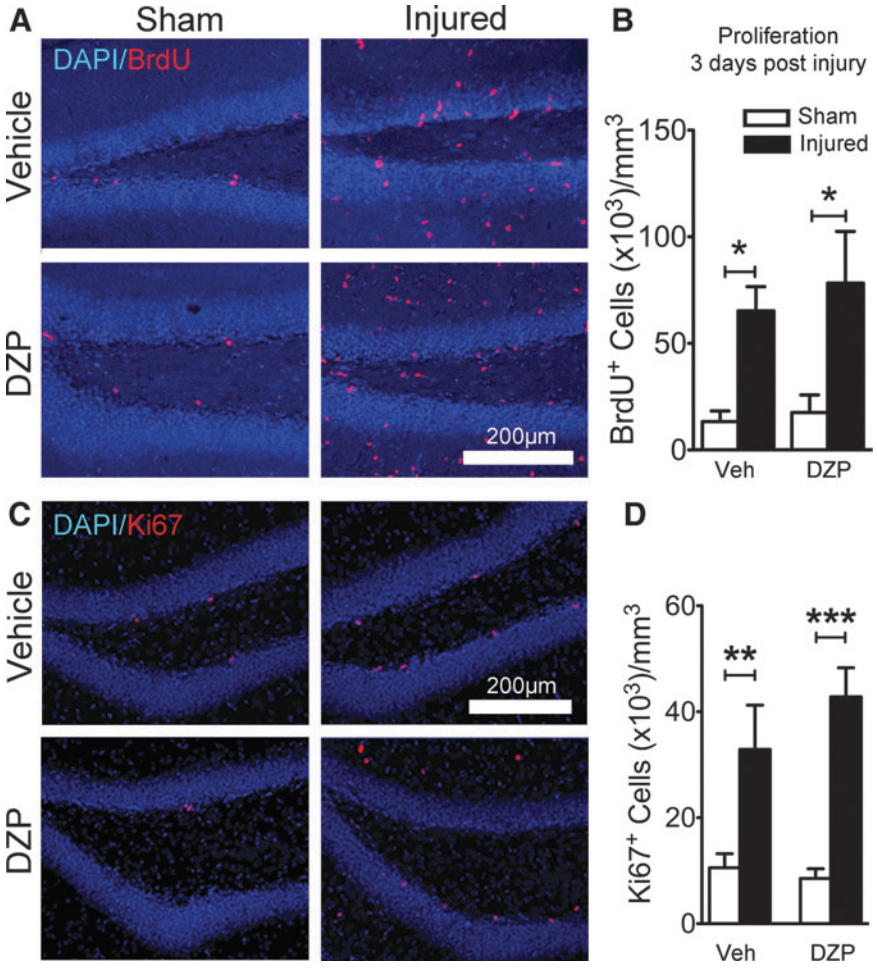

FIG. 2. Diazepam (DZP) does not affect cell proliferation early after controlled cortical impact (CCI). (A) BrdU-stained hippocampal tissue from sham and CCI-treated mice, exposed to either vehicle or DZP after sham/CCI. Mice were given BrdU 2 days after sham/CCI and fixed 1 day later to assess hippocampal cell proliferation. **(B)** Quantification of $BrdU^+$ cell density in the granule cell layer and subgranular zone of the dentate gyrus. Cell proliferation increased similarly in both vehicle- and DZP-exposed mice after injury (*$p < 0.05$ sham-vehicle vs. CCI-vehicle; sham-DZP vs. CCI-DZP, $n = 4$–6 mice/group). **(C)** Hippocampal sections stained for the cell proliferation marker Ki67 (red) treated with either vehicle or DZP, 3 days after sham or CCI. **(D)** Quantification of $Ki67^+$ cell density within the granule cell layer and subgranular zone of the dentate gyrus. Cell proliferation, as assessed by Ki67 expression, increased similarly in both vehicle- and DZP-exposed mice after injury (**$p < 0.01$ sham-vehicle vs. CCI-vehicle; ***$p < 0.001$ sham-DZP vs. CCI-DZP, $n = 8$–10 mice/group).

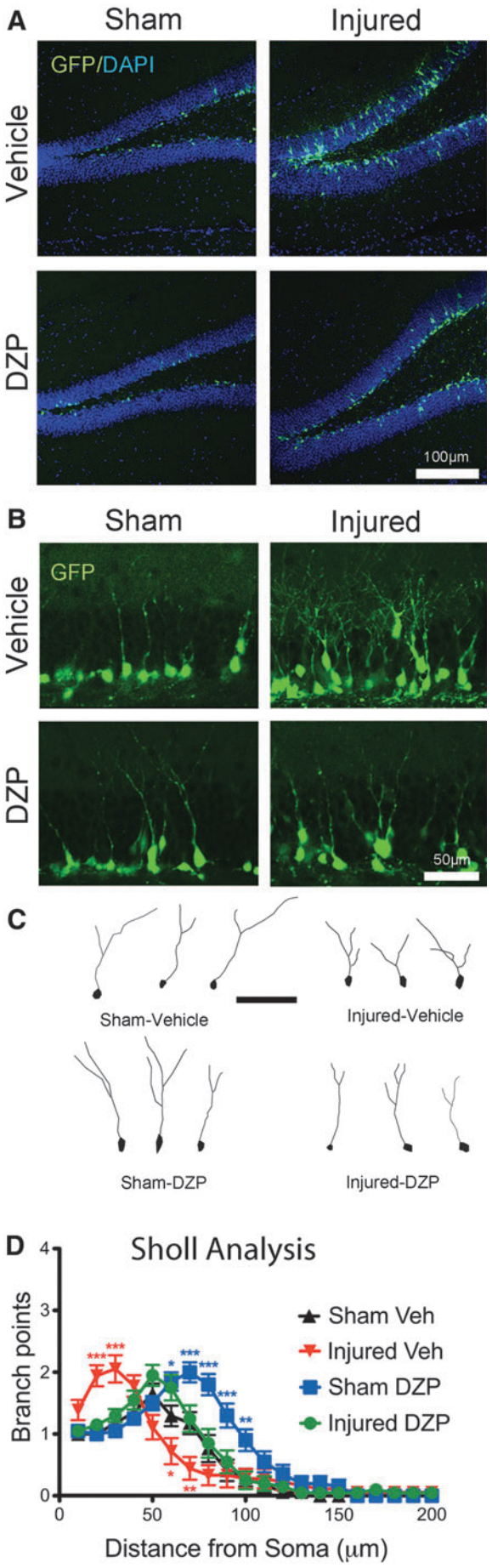

indicates cell proliferation.[52] CCI dramatically increased Ki67 expression in the GCL of the dentate gyrus (Fig. 2C,D). Ki67 expression increased similarly in both CCI-vehicle ($p=0.011$; vs. sham-vehicle; Mann-Whitney test; Fig. 2D) and CCI-DZP groups ($p=0.001$; vs. sham-DZP; Mann-Whitney test; Fig. 2D), and importantly, did not differ between CCI groups ($p=0.130$; CCI-vehicle vs. CCI-DZP; Mann-Whitney test; Fig. 2D). This observation further supports the lack of an effect of DZP on post-injury hippocampal cell proliferation. Again, DZP did not affect cell proliferation in sham-treated mice, as assayed by Ki67 expression ($p=0.515$; sham-vehicle vs. sham-DZP; Mann-Whitney test; Fig. 2C,D). Together, these data indicate that although DZP inhibits post-traumatic neurogenesis, this is not mediated by a DZP-induced decrease in cell proliferation.

Diazepam prevents aberrant dendritic arborization of neurons born after TBI

POMC-GFP mice transiently express GFP in immature (10- to 14-day-old) hippocampal adult-born neurons, and allow for morphological assessment of immature neurons.[42] Granule cells born after TBI exhibit dendritic branching abnormalities,[23,24] characterized by the increased branching of dendrites close to the soma and within the inner molecular layer. As dendritic outgrowth is modulated by $GABA_AR$ signaling during cell maturation,[33,53] we analyzed whether DZP affected the dendritic morphology of neurons born after CCI using hippocampal tissue from *POMC-GFP* mice 14 days after CCI or sham treatment.

We first examined the magnitude of post-traumatic neurogenesis in *POMC-GFP* mice treated with DZP. Consistent with our data from wild-type mice (Fig. 1B–E), CCI injury increased the densityof GFP^+ immature neurons in vehicle-treated *POMC-GFP* mice (sham-vehicle $=987\pm101$ cells/mm^2; CCI-vehicle $=1730\pm290$ cells/mm^2; $p=0.04$, Mann-Whitney test, $n=9$ mice/group; Fig. 3A,B), and the CCI-induced increase in GFP^+neuron density was inhibited by DZP (sham-DZP $=956\pm129$ cells/mm^2; CCI-

FIG. 3. Diazepam (DZP) inhibits post-traumatic neurogenesis and mitigates the effect of traumatic brain injury (TBI) on the dendritic morphology of adult-born neurons. **(A)** Representative images of the dentate gyrus of *POMC-GFP* mice 2 weeks after sham or controlled cortical impact (CCI) treatment, illustrating the increase in immature neuron (GFP^+) density following CCI in vehicle-treated but not DZP-treated mice. **(B)** Higher-power images demonstrating GFP^+ granule cell morphology after CCI or sham procedures in vehicle- and DZP-treated *POMC-GFP* mice. **(C)** Representative tracings of adult-born neurons from mice exposed to DZP or vehicle after CCI or sham treatment. **(D)** Sholl analysis comparing dendritic branching patterns of adult-born neurons generated in the different groups. Compared with sham-vehicle treatment (black line), adult-born neurons from injured mice treated with vehicle (red line) had more branches 20 μm and 30 μm from the soma, and had fewer branches 60 μm and 70 μm from the soma (red asterisks indicate comparison between CCI-vehicle and sham-vehicle,$^*p<0.05$, $^{**}p<0.01$, $^{***}p<0.001$). This injury-induced branching pattern was prevented by DZP, as there were no significant differences in the branching patterns between sham-vehicle and CCI-DZP treated mice (black vs. green lines). DZP alone enhanced distal branch length of new neurons in sham mice with no effects on proximal branching (blue asterisk indicates comparison between sham-DZP and sham-vehicle, $^*p<0.05$, $^{**}p<0.01$, $^{***}p<0.001$; compared with sham-vehicle) $n=17$–20 cells from 3–4 mice/group).

DZP = 1447 ± 219 cells/mm^2; $p = 0.72$, Mann-Whitney test, $n = 7$, 11 mice/group). Again, DZP had no effect on neurogenesis rate in non-injured *POMC-GFP* animals (sham-vehicle vs. sham-DZP; $p = 0.83$, Mann-Whitney test).

Morphological analysis of single GFP$^+$ neurons from sham and CCI-treated mice demonstrated that CCI altered the dendritic branching of neurons born after injury in vehicle-treated mice ($F[5.189, 171.238] = 6.587$; $p < 0.001$, CCI by distance interaction, sham-vehicle vs. CCI-vehicle, repeated measures ANOVA; Fig. 3C,D). CCI-induced adult-born neurons had more branches at proximal regions of their dendritic trees and fewer branches at more distal regions from the soma (20 μm, $p < 0.001$; 30 μm, $p < 0.001$; 60 μm, $p < 0.05$; 70 μm, $p < 0.01$; Bonferroni post hoc test; Fig. 3D), consistent with prior reports.[23,24] In contrast, aberrant proximal dendritic branching of neurons born after CCI was completely prevented by DZP treatment, which restored the normal (more distal) branching pattern of these cells and showed no difference from sham-vehicle controls in the the branching patterns at any single point (Fig. 3B–D).

Consistent with the previously described facilatory role of $GABA_AR$ activation on dendritic outgrowth,[29] DZP itself caused a mild but significant increase in dendritic length of immature neurons in sham-treated animals, with no effect on proximal branching patterns ($p > 0.05$ at 10–60 μm, $p < 0.001$ at 70 μm, 80 μm, and 90 μm, $p < 0.01$ at 100 μm, sham-vehicle vs. sham-DZP, Bonferroni post hoc test; $F[4.007, 140.245] = 5.656$; $p < 0.001$, drug by distance interaction, sham-vehicle vs. sham-DZP, repeated measures ANOVA, Fig. 3D). Also, as expected for neurons 10 to 14 days post-mitosis,[42] we did not observe dendritic spines on neurons in any treatment group. As dendritic spines begin to appear on immature neurons at approximately 16 days post-mitosis,[54] this suggests that neither CCI nor DZP treatments accelerated neuronal maturation in any group, and that no GFP$^+$ cells were generated prior to CCI/-sham procedures.

Diazepam does not attenuate the enhanced migration of adult-born neurons after TBI

Aberrant migration of adult-born neurons occurs after various forms of brain injury, including seizures, strokes, and TBI.[18,23–26,55] In our experiments here, neurons born after TBI also migrated greater distances from the SGZ (sham-vehicle vs. CCI-vehicle; $p = 0.0005$, Mann-Whitney test; Fig. 4A,B). However, in contrast to its other effects on post-injury neurogenesis, DZP did not prevent the aberrant migration of neurons born after CCI (sham-DZP vs. CCI-DZP treated mice; $p = 0.0007$, Mann-Whitney test; Fig. 4A,B). DZP also did not prevent the CCI-induced increase in ectopic cell migration into the dentate molecular layer (sham-vehicle vs. CCI-vehicle, $p = 0.003$; sham-DZP vs. CCI-DZP, $p = 0.002$; Mann-Whitney test; Fig. 4C, left) and actually enhanced the migration of a subset of adult-born neurons into the hilus (sham-DZP vs. CCI DZP; $p = 0.017$, Mann-Whitney test; Fig. 4C, right).

Diazepam does not alter neuronal injury, astroglial activation, or locomotor activity after CCI

The magnitude of post-traumatic neurogenesis is related to injury severity.[15,56] Thus, if DZP had neuroprotective effects, it could reduce post-traumatic neurogenesis indirectly through mitigation of the CCI injury. To assess for a potential effect of DZP on brain injury, we first assessed the degree of tissue damage 3 days after CCI. In brain sections at the epicenter of the CCI injury, there were no differences in the CCI-induced cortical cavity between vehicle- and DZP-treated mice ($p = 0.56$, Mann-Whitney test; Fig. 5A,B), indicating that DZP did not decrease the amount of cortex lost to injury.

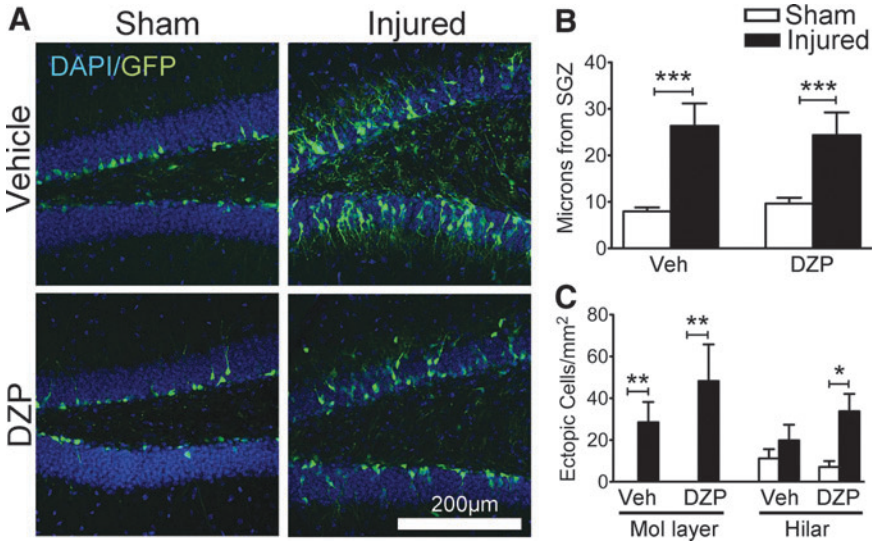

FIG. 4. Outward migration of adult-born neurons after controlled cortical impact (CCI) was not affected by diazepam (DZP). **(A)** Images of the dentate gyrus from *POMC-GFP* mice illustrate the migration of adult-born neurons away from the subgranular zone (SGZ) in sham and injured mice treated with DZP or vehicle. **(B)** Quantification of migration distance of adult-born neurons from the SGZ. GFP$^+$ neurons generated after injury migrated greater distances from the SGZ compared with those born under sham conditions, and this was not prevented by DZP (***$p < 0.001$; $n = 7$–11 mice/group). **(C)** Quantification of ectopic adult-born neuron migration into the hilus or molecular layer of the dentate gyrus. CCI increased the number of ectopically migrated adult-born neurons in the molecular layer similarly in both vehicle- or DZP-exposed mice (**$p < 0.01$; $n = 7$–11 mice/group; left). Injured mice treated with DZP actually had a greater density of adult-born neurons in the hilus compared with their sham-DZP treated control group (*$p < 0.05$), whereas injured mice not treated with DZP were no different from their sham-vehicle treated control group ($p = 0.61$; sham-vehicle vs. CCI-vehicle treated mice; $n = 7$–11 mice/group; right).

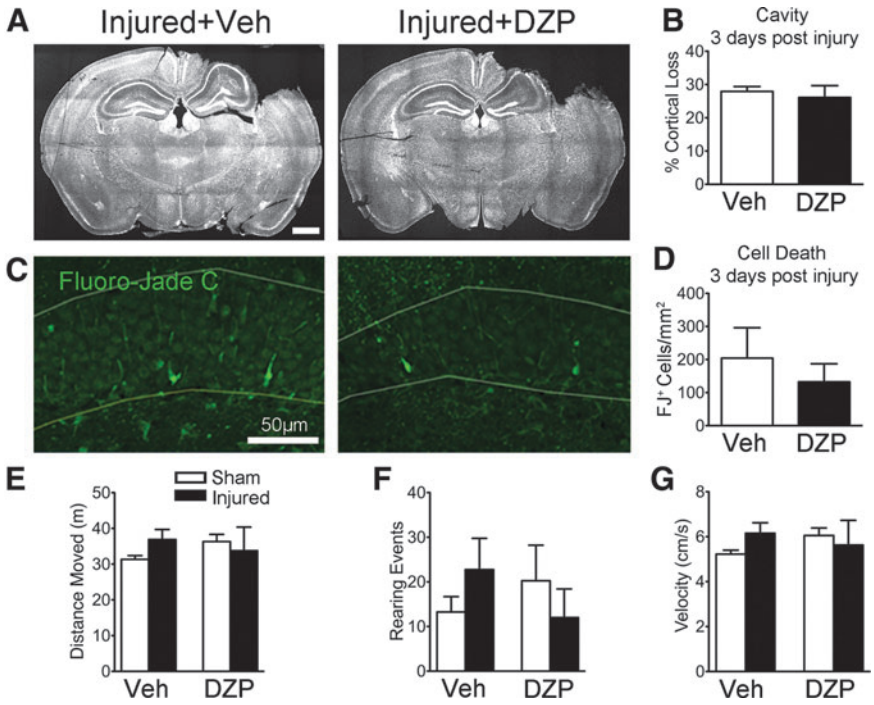

FIG. 5. Diazepam (DZP) does not decrease neuronal injury or alter locomotoractivity after controlled cortical impact (CCI). **(A)** Images depicting typical cortical injuries in mice exposed to vehicle or DZP. Scale bar: 1 mm. **(B)** Quantification of cortical loss after injury. There were no differences between vehicle- and DZP-treated mice ($p = 0.56$, $n = 6$–10 mice/group). **(C)** Fluoro-Jade C staining of degenerating cells in the dentate granule cell layer from injured mice exposed to vehicle or DZP. **(D)** Quantification of Fluoro-Jade-C$^+$ cell density in the granule cell layer of the dentate gyrus, 3 days after injury. There were no differences in the density of Fluoro-Jade C$^+$ cells between injured mice exposed to vehicle and DZP treatment ($n = 9$–11 mice/group). **(E)** Open field analysis performed 3 days after sham or CCI demonstrates that mice moved similar distances in the 10-min session in all groups, independent of vehicle versus DZP treatment ($p = 0.809$, effect of drug, $n = 4$ mice/group). **(F)** Rearing events during the open field testing did not differ in frequency between groups ($p = 0.916$). **(G)** Open field mean velocities from distance traveled also did not differ between groups ($p = 0.809$).

As this gross anatomical measurement might not be sensitive to cell death within the parenchyma, we examined cell death with Fluoro-Jade C after CCI in both vehicle- and DZP-treated mice 3 days after injury. There was no difference in cell death between CCI-injured mice given vehicle versus DZP (Fig. 5C–D). We also examined a separate cohort of injured brains 3 h after injury, and again found no differences in the density of Fluoro-Jade C$^+$ cells between DZP- and vehicle-treated mice in either the GCL (vehicle, 54.5 ± 13.9 cells/μm^2; DZP, 19.7 ± 6.3 cells/μm^2; $p = 0.11$, Mann-Whitney test, $n = 4$ mice/group) or peri-lesional cortex (vehicle, 1075 ± 334 cells/μm^2; DZP, 1248 ± 140 cells/μm^2; $p = 0.49$, Mann-Whitney test, $n = 4$ mice/group).

As neurogenesis is enhanced by locomotor activity,[62] we assayed whether DZP may have altered post-injury neurogenesis by reducing mouse locomotor activity levels. First, gross daily observation of mice did not reveal any sedating effects of our DZP dose in either CCI- or sham-treated mice (data not shown). However, as gross observations rely on qualitative assessments, we quantified open field activity in mice 3 days after injury, to coincide with the time-point used for our analyses of neurogenesis/mitosis. DZP did not alter locomotor activity of mice after CCI, based on the lack of group differences in the total distance moved ($p = 0.809$, effect of drug; two-way ANOVA, $n = 4$ mice/group; Fig. 5E); rearing events ($p = 0.916$, vehicle vs. drug; Mann-Whitney test; Fig. 5F); or in mean velocity ($p = 0.809$, effect of drug; two-way ANOVA; Fig. 5G). These data indicate that differences in locomotor activity do not account for DZP's specific effects on post-injury neurogenesis.

Astroglia are activated by neuronal injury and can release factors that modulate the survival and maturation of adult-born neurons.[57–59] Astroglia also express benzodiazepine-sensitive GABA$_A$Rs, which can modulate glial activation.[60] Thus, if DZP altered glial function after injury, either by directly modulating glial activation or glial proliferation, or by reducing post-injury signaling to astroglia, it could affect post-injury neurogenesis through DZP-induced changes in astroglial function.

To assess astroglial activation, we stained hippocampal sections for the acute phase marker glial fibrillary acidic protein (GFAP), which increases in expression during glial activation. As has been commonly observed,[15,61] CCI increased the density of GFAP immunofluorescence when compared with sham-treated mice receiving vehicle ($p = 0.029$; sham-vehicle vs. CCI vehicle; Mann-Whitney test; Fig. 6A,B). This increase in GFAP staining after CCI was similar in DZP-treated animals ($p = 0.0087$; sham-DZP vs. CCI-DZP; Mann-Whitney test; Fig. 6A,B), and was not different between CCI-vehicle and CCI-DZP treated mice ($p = 0.413$, Mann-Whitney test). The data not only indicate that astroglial activation was not reduced by DZP, but also provide further evidence that injury magnitude was not affected by DZP.

Additionally, mice were weighed just before and 1 week after DZP exposure to globally assess the potential of DZP-induced weight changes, which could indicate other effects on mouse health

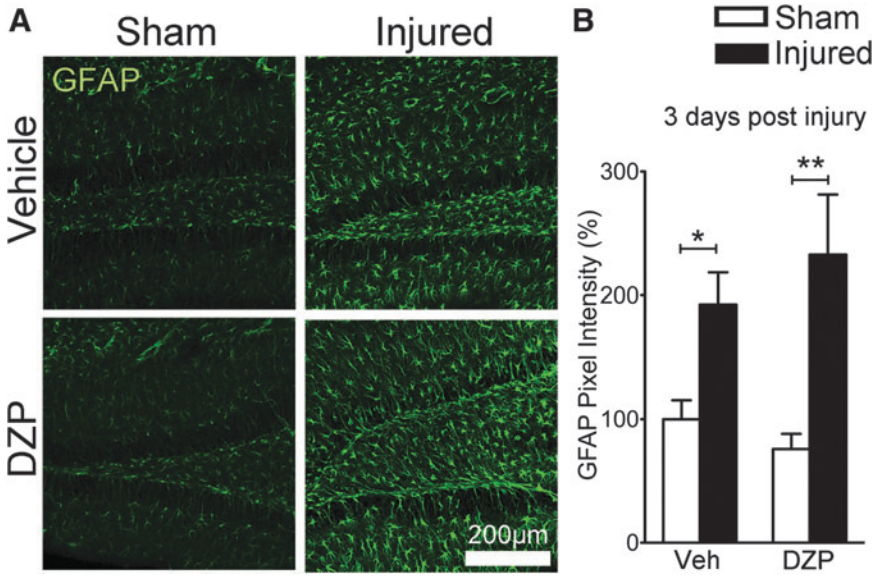

FIG. 6. Diazepam (DZP) does not attenuate glial activation after controlled cortical impact (CCI). **(A)** Images of glial fibrilary acidic protein (GFAP)-stained hippocampal tissue from sham- or CCI-treated mice exposed to vehicle or DZP. **(B)** Quantification of GFAP immunoreactivity within the dentate gyrus (molecular layer and hilar pixel intensities were combined, as there were no regional differences), normalized to mean pixel intensity of sham/vehicle-treated sections. CCI injury increased GFAP intensity irrespective of drug treatment (*$p < 0.05$, sham-vehicle vs. CCI-vehicle; **$p < 0.01$, sham-DZP vs. CCI-DZP, $n = 4$–6 mice/group).

or nutritional status. Although post-injury weight gain was slightly lower in both groups of CCI-treated mice, mouse weight was unaffected by DZP (change in weight during the week of pump exposure: sham-vehicle = 0.68 ± 0.14 g; CCI-vehicle = 0.44 ± 0.29 g; sham-DZP = 1.09 ± 0.26 g; CCI-DZP = 0.26 ± 0.16 g; two-way ANOVA, $F[1,25] = 4.242$, $p = 0.0499$ main effect of CCI; $p = 0.666$ for effect of DZP, $n = 7$ mice/group).

Diazepam inhibits the injury-induced burst of neuronal activity in the dentate gyrus

TBI induces dramatic changes in neuronal activity, both directly at the time of injury, and in subsequent weeks due to neuronal death and dysfunction.[23,63] In humans, TBI can cause clinical or subclinical seizures at or near the time of injury.[64] As neuronal activity and seizures can positively modulate neurogenesis,[32,65,66] we postulated that DZP might reduce post-traumatic neurogenesis by reducing neuronal activity. To assay neuronal activity during the early post-injury period, we stained hippocampi from CCI- and sham-treated mice for the activity-dependent gene c-Fos.

As previously described,[15,67,68] injury transiently increased neuronal activity in the hippocampal dentate gyrus in vehicle-exposed mice within hours after injury (Fig. 7A,B; $p = 0.029$, Mann-Whitney test, $n = 4$/group). At this same time-point, DZP-treated mice did not demonstrate a statistically significant increase in c-Fos$^+$ expression after CCI (Fig. 7A,B; $p = 0.40$, Mann-Whitney test, $n = 3$, 3–4 mice) indicating that DZP had attenuated the early injury-induced burst of hippocampal neural activity, shortly after osmotic pump implantation.

Three days after injury, DZP caused an overall reduction of neuronal activity within the GCL of mice in both sham and CCI groups, as quantified using c-Fos$^+$ cell density ($F[1,33] = 25.63$, $p = 0.00002$; main effect of drug, two-way ANOVA; Fig. 7C,D,F). Independently, CCI was associated with reduced c-Fos$^+$ activation in the dentate gyrus in both drug treatment groups ($F[1,33] = 13.2$, $p = 0.0009$; main effect of CCI, two-way ANOVA; Fig. 7E), which may be the immunohistochemical manifestation of post-traumatic neural depression that has been described in both humans and animals after TBI.[69] Thus, at both early and late phases after injury, DZP inhibited neuronal activity throughout the dentate gyrus, which was associated with both quantitative and qualitative normalization of post-traumatic neurogenesis.

Discussion

DZP prevented post-traumatic neurogenesis and inhibited the aberrant dendritic development of neurons born after TBI. This not only has implications for our mechanistic understanding of injury-induced neurogenesis, but will facilitate future investigation into the importance of post-traumatic neurogenesis to recovery after brain injury.

Activity-dependent mechanisms in neurogenesis

Constitutive neurogenesis is strongly regulated by network activity, as environmental/behavioral contingencies and the direct activation of neurotransmitter-binding receptors can increase the proliferation of stem cells and survival of adult born neurons.[32,66,70–73] Thus, it is plausible that these mechanisms could sculpt the neurogenic response after injury as well. TBIs are known to induce seizure-like activity early after injury,[74] and seizures increase neurogenesis and alter the dendritic structure of adult-born neurons.[26,27] Thus, the inhibition of post-traumatic neurogenesis by DZP could be due to inhibition of circuit hyperactivity after injury, and in particular via suppression of sub-clinical seizure activity after TBI. Although we did not directly measure seizure activity after CCI in our mice, our c-fos staining indicated that DZP reduced activity during both early and late phases after injury, consistent with the known seizure-suppressing effects of benzodiazepines.[75]

Our finding that DZP normalized the dendritic development of cells generated after injury is surprising, due to the time course of

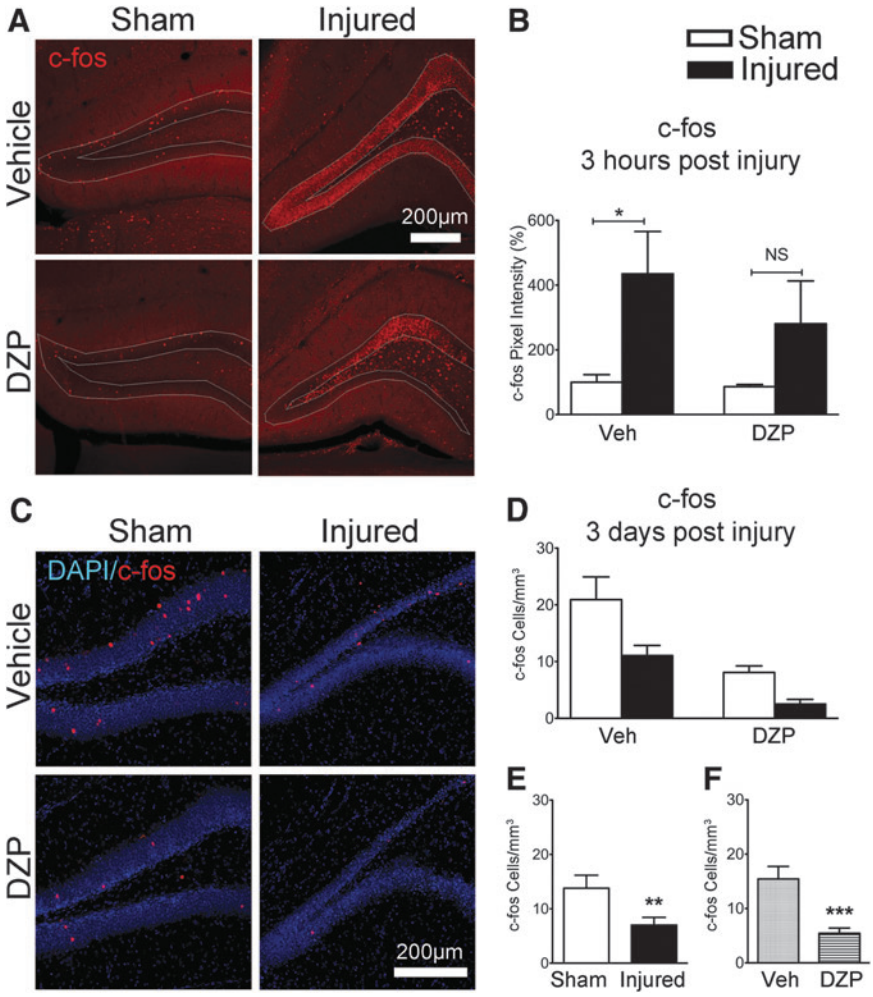

FIG. 7. Diazepam (DZP) reduces neuronal activity after CCI. **(A)** Images of the dentate gyrus of sham or injured mice treated with DZP or vehicle, 3 h after treatment. White lines delineate the traced granule cell layer (GCL) used for quantification. **(B)** Mean pixel intensity of c-fos immunoreactivity within the GCL, normalized to mean pixel intensity of sham/vehicle-treated sections. Injury significantly increased c-fos expression in vehicle-treated, but not DZP-treated, mice ($*p<0.05$, sham-vehicle vs. CCI-vehicle; $p=0.40$; sham-DZP vs. CCI-DZP, $n=3$–4 mice per group). **(C)** c-Fos staining (red) in the dentate gyrus of sham-and CCI-injured mice treated with DZP or vehicle, 3 days after sham or CCI injury. DAPI (blue) shows the outline of the GCL of the dentate gyrus. **(D)** Quantification of c-fos$^+$ cell density. **(E)** c-fos$^+$ cell density was reduced by CCI injury independent of drug treatment ($**p<0.001$) and by **(F)** DZP independent of CCI treatment ($***p<0.0001$; $n=8$–10 mice/group).

drug administration relative to dendritic outgrowth. DZP was removed after the first post-injury week, before the majority of the dendritic outgrowth by this population of cells would have occurred,[54] yet the cells still exhibited dendritic branching patterns that were similar to cells born in uninjured brains. This suggests that DZP induced longer-lasting changes in the hippocampal signaling environment, or caused other changes in gene expression in these neurons[76] that persisted after DZP exposure ended.

DZP blocked post-traumatic neurogenesis without affecting the early burst of cell proliferation after injury, and inhibited the aberrant dendritic development of these cells without preventing their enhanced outward migration. Thus, our data suggest that post-traumatic neurogenesis is influenced by multiple different signals, which drive both an early hyperproliferative response as well as subsequent alterations in neuronal survival, cell migration, and dendritic arborization. As glial activation and neuronal cell death were unaffected by DZP, we propose that glial-derived or other injury-related signals drive the increase in hippocampal stem cell proliferation,[23,77–81] after which neuronal activity or $GABA_AR$-mediated signaling is required for the successful maturation of these cells into neurons. This is consistent with the notion that survival signaling can involve both an activity-independent early phase and an activity-dependent late phase.[45,50,82,83] Similarly, our observation that DZP does not block the TBI-induced migration of adult-born cells suggests that migration of these cells after injury is controlled by other injury-induced alterations in signaling gradients, such as reelin, which were not affected by DZP.

Finally, it must be noted that although we found an association between the DZP-induced reduction in neuronal activity and the normalization of neurogenesis, our work does not establish a causal relationship between these two observations. Although this would be difficult to prove *in vivo*, we suspect that further studies of the specific signaling mechanisms involved will shed light on this question.

$GABA_AR$-mediated modulation of neurogenesis

DZP could also have directly affected the survival of adult-born neurons by modulating $GABA_ARs$ on individual adult-born neurons in a cell-autonomous manner. Functional $GABA_ARs$ are expressed on the membranes of neuronal precursor cells and radial glial cells,[39,84] and DZP, a $GABA_AR$ allosteric modulator, could increase signaling via those receptors. Although $GABA_ARs$ control the rate of adult-born neuron maturation and dendritic outgrowth,[33] data suggesting that $GABA_AR$ activity directly modulates cell proliferation and survival are less clear.

Prior studies have obtained conflicting results regarding the effects of DZP on neurogenesis rates in healthy animals, with either no or minimal effect,[85–87] an increase in cell proliferation,[40] or a net decrease in neurogenesis.[39,72] In apparent contrast to results obtained by Song and colleagues,[39] we did not observe an effect of DZP in sham-treated animals, although we employed a different dosing strategy (continuous administration vs. once-daily i.p. injection). We chose to administer DZP via pump given the short ($\sim$ 1 h) half-life of DZP in rodents,[47,88] and to model continuous drug administration, as might be expected for humans receiving prolonged sedative infusions during post-injury intensive care. These different dosing strategies drive differential gene expression patterns *in vivo,*[89] and thus could explain this discrepancy.

Our results are reminiscent of a recent study in which DZP completely prevented the early phases of post-ischemic neurogenesis when administered for just 3 days after stroke.[87] This study, however, did not examine cells after neuronal differentiation and early maturation had commenced, so it is unclear whether other aspects of post-ischemic neurogenesis, such as the aberrant maturation of adult-born granule cells,[25] were also affected.

Future work will hopefully determine whether the effect of DZP on adult-born granule cells is cell autonomous or mediated by changes in network activity. In this regard, it would be of interest to determine whether other $GABA_AR$ agonists used in the management of acute head injury, such as propofol or etomidate, have similar effects on post-injury neurogenesis during prolonged administration, as they modulate $GABA_ARs$ at different binding sites and have different off-target effects.[90,91]

Implications for functional recovery

Although neurons born after TBI likely contribute to hippocampal information processing after injury,[23] it is unknown whether increased neurogenesis is beneficial or maladaptive, particularly given the abnormal morphology and aberrant migration of cells born after injury.[23,24] Because neurons born after other brain injuries aberrantly integrate into the hippocampal network[25,26] and might play a role in driving neuropathology,[29] it is possible that aberrantly developed neurons could drive long-term circuit dysfunction after TBI, for example, by driving hippocampal hyperexcitability and post-traumatic epilepsy, or via depletion of the stem cell pool.[30,92]

Previous attempts to assess the functional significance of post-traumatic neurogenesis have done so via genetic or pharmacological inhibition of neurogenesis, followed by behavioral assessment of cognitive performance.[93,94] However, these studies inhibited neurogenesis below baseline levels, which alone causes cognitive impairments.[8,95–97] An alternative approach has involved the administration of growth factors to increase neurogenesis after TBI[20,21,98–100]; however, growth factors can modulate other neuronal functions, such as synaptic plasticity.[101] As DZP appeared to normalize post-traumatic neurogenesis both quantitatively and qualitatively, it will facilitate analysis of whether the alterations in neurogenesis after TBI positively or negatively affect long-term outcomes.

The contribution of hippocampal neurogenesis to recovery after human TBI is unknown. Although hippocampal neurogenesis has been demonstrated in adult humans using a variety of different techniques,[7,102–104] there is a lack of data on human neurogenesis after TBI, which likely results from difficulty in obtaining samples at the appropriate post-injury interval. One study examined pediatric brains after TBI with a very short, mean post-injury survival of just 33 h, and did not see evidence of increased neurogenesis.[105] However, this is before increased neurogenesis is observed in rodent models[106] and thus, these samples may have been obtained before the initiation of post-injury neurogenesis. Interestingly, the one sample from this study obtained 7 days after injury demonstrated a notable increase in hippocampal neurogenesis. As histochemical studies have inherent limitations due to tissue availability and processing, perhaps non-invasive quantification of neurogenesis[107]could one day conclusively characterize the course of post-injury neurogenesis in humans.

Acknowledgments

This material was supported in part by the Department of Veterans Affairs, Veterans Health Administration, Office of Research and Development, Biomedical Laboratory Research and Development CDA-2 Award 005-10S (ES), a Department of Veterans Affairs Merit Review Award I01-BX002949 (ES), a Department of Defense CDMRP Award W81XWH-18-1-0598 (ES), the Oregon Clinical and Translational Research Institute (OCTRI) NIH TL1TR000129 from the National Center for Advancing Translational Sciences at the National Institutes of Health (RM), the NIH F32NS083109 (LEV), a BIRCWH K12HD043488 Award made possible through the Eunice Kennedy Shriver National Institute of Child Health and Human Development and the Office of Research on Women's Health (LEV), and P30NS061800 (OHSU) Awards. We thank Dr. Gary Westbrook of the Vollum Institute for comments on our manuscript, Dr. Stefanie Kaech-Petrie of the OHSU Advanced Light Microscopy Core for assistance with imaging, and our lab volunteer Khanh Doan and research assistants Sarah Mader and Alexandria Wilson for outstanding technical support. The contents of this manuscript do not represent the views of the U.S. Department of Veterans Affairs or the United States Government.

Author Disclosure Statement

No competing financial interests exist.

References

1. CDC: Rates of TBI-related Emergency Department Visits, Hospitalizations, and Deaths by Sex—United States, 2001–2010 | Concussion | Traumatic Brain Injury | CDC Injury Center [online]. www.cdc.gov/traumaticbraininjury/data/rates_bysex.html (Last accessed March 23, 2018).
2. Draper, K., and Ponsford, J. (2008). Cognitive functioning ten years following traumatic brain injury and rehabilitation. Neuropsychology 22, 618–625.
3. Arciniegas, D.B., Held, K., and Wagner, P. (2002). Cognitive impairment following traumatic brain injury. Curr. Treat. Options Neurol. 4, 43–57.
4. Jorge, R.E., Robinson, R.G., Moser, D., Tateno, A., Crespo-Facorro, B., and Arndt, S. (2004). Major depression following traumatic brain injury. Arch. Gen. Psychiatry 61, 42–50.
5. Fleminger, S. (2008). Long-term psychiatric disorders after traumatic brain injury. Eur. J. Anaesthesiol., Suppl 42, 123–130.

6. Altman, J., and Das, G.D. (1965). Autoradiographic and histological evidence of postnatal hippocampal neurogenesis in rats. J. Comp. Neurol. 124, 319–335.
7. Eriksson, P.S., Perfilieva, E., Bjork-Eriksson, T., Alborn, A.M., Nordborg, C., Peterson, D.A., and Gage, F.H. (1998). Neurogenesis in the adult human hippocampus. Nat. Med. 4, 1313–1317.
8. Clelland, C.D., Choi, M., Romberg, C., Clemenson, G.D., Jr., Fragniere, A., Tyers, P., Jessberger, S., Saksida, L.M., Barker, R.A., Gage, F.H., and Bussey, T.J. (2009). A functional role for adult hippocampal neurogenesis in spatial pattern separation. Science 325, 210–213.
9. Nakashiba, T., Cushman, J.D., Pelkey, K.A., Renaudineau, S., Buhl, D.L., McHugh, T.J., Rodriguez Barrera, V., Chittajallu, R., Iwamoto, K.S., McBain, C.J., Fanselow, M.S., and Tonegawa, S. (2012). Young dentate granule cells mediate pattern separation, whereas old granule cells facilitate pattern completion. Cell 149, 188–201.
10. Shors, T.J., Miesegaes, G., Beylin, A., Zhao, M., Rydel, T., and Gould, E. (2001). Neurogenesis in the adult is involved in the formation of trace memories. Nature 410, 372–376.
11. Jacobs, B.L., van Praag, H., and Gage, F.H. (2000). Adult brain neurogenesis and psychiatry: a novel theory of depression. Mol. Psychiatry 5, 262–269.
12. Santarelli, L., Saxe, M., Gross, C., Surget, A., Battaglia, F., Dulawa, S., Weisstaub, N., Lee, J., Duman, R., Arancio, O., Belzung, C., and Hen, R. (2003). Requirement of hippocampal neurogenesis for the behavioral effects of antidepressants. Science 301, 805–809.
13. Dash, P.K., Mach, S.A., and Moore, A.N. (2001). Enhanced neurogenesis in the rodent hippocampus following traumatic brain injury. J. Neurosci. Res. 63, 313–319.
14. Sun, D., McGinn, M.J., Zhou, Z., Harvey, H.B., Bullock, M.R., and Colello, R.J. (2007). Anatomical integration of newly generated dentate granule neurons following traumatic brain injury in adult rats and its association to cognitive recovery. Exp. Neurol. 204, 264–272.
15. Villasana, L.E., Westbrook, G.L., and Schnell, E. (2014). Neurologic impairment following closed head injury predicts post-traumatic neurogenesis. Exp. Neurol. 261, 156–162.
16. Chirumamilla, S., Sun, D., Bullock, M.R., and Colello, R.J. (2002). Traumatic brain injury induced cell proliferation in the adult mammalian central nervous system. J. Neurotrauma 19, 693–703.
17. Kernie, S.G., Erwin, T.M., and Parada, L.F. (2001). Brain remodeling due to neuronal and astrocytic proliferation after controlled cortical injury in mice. J. Neurosci. Res. 66, 317–326.
18. Rice, A.C., Khaldi, A., Harvey, H.B., Salman, N.J., White, F., Fillmore, H., and Bullock, M.R. (2003). Proliferation and neuronal differentiation of mitotically active cells following traumatic brain injury. Exp. Neurol. 183, 406–417.
19. Chohan, M.O., Bragina, O., Kazim, S.F., Statom, G., Baazaoui, N., Bragin, D., Iqbal, K., Nemoto, E., and Yonas, H. (2014). Enhancement of neurogenesis and memory by a neurotrophic peptide in mild to moderate traumatic brain injury. Neurosurgery 76, 201–214; discussion 214–215.
20. Lu, D., Mahmood, A., Qu, C., Goussev, A., Schallert, T., and Chopp, M. (2005). Erythropoietin enhances neurogenesis and restores spatial memory in rats after traumatic brain injury. J. Neurotrauma 22, 1011–1017.
21. Lu, D., Mahmood, A., Zhang, R., Li, Y., and Chopp, M. (2003). Upregulation of neurogenesis and reduction in functional deficits following administration of DETA/NONOate, a nitric oxide donor, after traumatic brain injury in rats. J. Neurosurg. 99, 351–361.
22. Xie, C., Cong, D., Wang, X., Wang, Y., Liang, H., Zhang, X., and Huang, Q. (2014). The effect of simvastatin treatment on proliferation and differentiation of neural stem cells after traumatic brain injury. Brain Res. 1602, 1–8.
23. Villasana, L.E., Kim, K.N., Westbrook, G.L., and Schnell, E. (2015). Functional Integration of Adult-Born Hippocampal Neurons after Traumatic Brain Injury(1,2,3). eNeuro 2, pii: ENEURO.0056-15.2015.
24. Ibrahim, S., Hu, W., Wang, X., Gao, X., He, C., and Chen, J. (2016). Traumatic brain injury causes aberrant migration of adult-born neurons in the hippocampus. Sci. Rep. 6, 21793.
25. Niv, F., Keiner, S., Krishna-, Witte, O.W., Lie, D.C., and Redecker, C. (2012). Aberrant neurogenesis after stroke: a retroviral cell labeling study. Stroke 43, 2468–2475.
26. Overstreet-Wadiche, L.S., Bromberg, D.A., Bensen, A.L., and Westbrook, G.L. (2006). Seizures accelerate functional integration of adult-generated granule cells. J. Neurosci. 26, 4095–4103.
27. Jessberger, S., Zhao, C., Toni, N., Clemenson, G.D., Jr., Li, Y., and Gage, F.H. (2007). Seizure-associated, aberrant neurogenesis in adult rats characterized with retrovirus-mediated cell labeling. J. Neurosci. 27, 9400–9407.
28. Danzer, S.C. (2012). Depression, stress, epilepsy and adult neurogenesis. Exp. Neurol. 233, 22–32.
29. Parent, J.M., Jessberger, S., Gage, F.H., and Gong, C. (2007). Is neurogenesis reparative after status epilepticus? Epilepsia 48, Suppl. 8, 69–71.
30. Neuberger, E.J., Swietek, B., Corrubia, L., Prasanna, A., and Santhakumar, V. (2017). Enhanced dentate neurogenesis after brain injury undermines long-term neurogenic potential and promotes seizure susceptibility. Stem Cell Rep. 9, 972–984.
31. Gould, E., McEwen, B.S., Tanapat, P., Galea, L.A., and Fuchs, E. (1997). Neurogenesis in the dentate gyrus of the adult tree shrew is regulated by psychosocial stress and NMDA receptor activation. J. Neurosci. 17, 2492–2498.
32. Tashiro, A., Sandler, V.M., Toni, N., Zhao, C., and Gage, F.H. (2006). NMDA-receptor-mediated, cell-specific integration of new neurons in adult dentate gyrus. Nature 442, 929–933.
33. Ge, S., Goh, E.L., Sailor, K.A., Kitabatake, Y., Ming, G.L., and Song, H. (2006). GABA regulates synaptic integration of newly generated neurons in the adult brain. Nature 439, 589–593.
34. Duveau, V., Laustela, S., Barth, L., Gianolini, F., Vogt, K.E., Keist, R., Chandra, D., Homanics, G.E., Rudolph, U., and Fritschy, J.M. (2011). Spatiotemporal specificity of GABAA receptor-mediated regulation of adult hippocampal neurogenesis. Eur. J. Neurosci. 34, 362–373.
35. Pallotto, M., Nissant, A., Fritschy, J.M., Rudolph, U., Sassoe-Pognetto, M., Panzanelli, P., and Lledo, P.M. (2012). Early formation of GABAergic synapses governs the development of adult-born neurons in the olfactory bulb. J. Neurosci. 32, 9103–9115.
36. Li, Y., Aimone, J.B., Xu, X., Callaway, E.M., and Gage, F.H. (2012). Development of GABAergic inputs controls the contribution of maturing neurons to the adult hippocampal network. Proc. Natl. Acad. Sci. U S A 109, 4290–4295.
37. Garcia, P.S., Kolesky, S.E., and Jenkins, A. (2010). General anesthetic actions on GABA(A) receptors. Curr. Neuropharmacol. 8, 2–9.
38. Flower, O., and Hellings S. (2012). Sedation in traumatic brain injury. Emerg. Med. Int. 2012, 637171.
39. Song, J., Zhong, C., Bonaguidi, M.A., Sun, G.J., Hsu, D., Gu, Y., Meletis, K., Huang, Z.J., Ge, S., Enikolopov, G., Deisseroth, K., Luscher, B., Christian, K.M., Ming, G.L., and Song, H. (2012). Neuronal circuitry mechanism regulating adult quiescent neural stem-cell fate decision. Nature 489, 150–154.
40. Petrus, D.S., Fabel, K., Kronenberg, G., Winter, C., Steiner, B., and Kempermann, G. (2009). NMDA and benzodiazepine receptors have synergistic and antagonistic effects on precursor cells in adult hippocampal neurogenesis. Eur. J. Neurosci. 29, 244–252.
41. Krzisch, M., Sultan, S., Sandell, J., Demeter, K., Vutskits, L., and Toni, N. (2013). Propofol anesthesia impairs the maturation and survival of adult-born hippocampal neurons. Anesthesiology 118, 602–610.
42. Overstreet, L.S., Hentges, S.T., Bumaschny, V.F., de Souza, F.S., Smart, J.L., Santangelo, A.M., Low, M.J., Westbrook, G.L., and Rubinstein, M. (2004). A transgenic marker for newly born granule cells in dentate gyrus. J. Neurosci. 24, 3251–3259.
43. Brody, D.L., Mac Donald, C., Kessens, C.C., Yuede, C., Parsadanian, M., Spinner, M., Kim, E., Schwetye, K.E., Holtzman, D.M., and Bayly, P.V. (2007). Electromagnetic controlled cortical impact device for precise, graded experimental traumatic brain injury. J. Neurotrauma 24, 657–673.
44. Cameron, H.A., and McKay, R.D. (2001). Adult neurogenesis produces a large pool of new granule cells in the dentate gyrus. J. Comp. Neurol. 435, 406–417.
45. Dayer, A.G., Ford, A.A., Cleaver, K.M., Yassaee, M., and Cameron, H.A. (2003). Short-term and long-term survival of new neurons in the rat dentate gyrus. J. Comp. Neurol. 460, 563–572.
46. Depino, A.M., Tsetsenis, T., and Gross, C. (2008). GABA homeostasis contributes to the developmental programming of anxiety-related behavior. Brain Res. 1210, 189–199.
47. Friedman, H., Abernethy, D.R., Greenblatt, D.J., and Shader, R.I. (1986). The pharmacokinetics of diazepam and desmethyldiazepam in rat brain and plasma. Psychopharmacology (Berl.) 88, 267–270.
48. Klotz, U., Antonin, K.H., and Bieck, P.R. (1976). Pharmacokinetics and plasma binding of diazepam in man, dog, rabbit, guinea pig and rat. J. Pharmacol. Exp. Ther. 199, 67–73.

49. Richardson, R.M., Sun, D., and Bullock, M.R. (2007). Neurogenesis after traumatic brain injury. Neurosurg. Clin. N. Am. 18, 169–181, xi.
50. Kempermann, G., Gast, D., Kronenberg, G., Yamaguchi, M., and Gage, F.H. (2003). Early determination and long-term persistence of adult-generated new neurons in the hippocampus of mice. Development 130, 391–399.
51. Pathania, M., Yan, L.D., and Bordey, A. (2010). A symphony of signals conducts early and late stages of adult neurogenesis. Neuropharmacology 58, 865–876.
52. Scholzen, T., and Gerdes J. (2000). The Ki-67 protein: from the known and the unknown. J. Cell Physiol. 182, 311–322.
53. Sernagor, E., Chabrol, F., Bony, G., and Cancedda, L. (2010). GABAergic control of neurite outgrowth and remodeling during development and adult neurogenesis: general rules and differences in diverse systems. Front. Cell Neurosci. 4, 11.
54. Zhao, C., Teng, E.M., Summers, R.G., Jr., Ming, G.L., and Gage, F.H. (2006). Distinct morphological stages of dentate granule neuron maturation in the adult mouse hippocampus. J. Neurosci. 26, 3–11.
55. Parent, J.M., Elliott, R.C., Pleasure, S.J., Barbaro, N.M., and Lowenstein, D.H. (2006). Aberrant seizure-induced neurogenesis in experimental temporal lobe epilepsy. Ann. Neurol. 59, 81–91.
56. Wang, X., Gao, X., Michalski, S., Zhao, S., and Chen, J. (2016). Traumatic brain injury severity affects neurogenesis in adult mouse hippocampus. J. Neurotrauma 33, 721–733.
57. Sultan, S., Li, L., Moss, J., Petrelli, F., Casse, F., Gebara, E., Lopatar, J., Pfrieger, F.W., Bezzi, P., Bischofberger, J., and Toni, N. (2015). Synaptic integration of adult-born hippocampal neurons is locally controlled by astrocytes. Neuron 88, 957–972.
58. Morrens, J., Van Den Broeck, W., and Kempermann, G. (2012). Glial cells in adult neurogenesis. Glia 60, 159–174.
59. Lu, Z., and Kipnis, J. (2010). Thrombospondin 1—a key astrocyte-derived neurogenic factor. FASEB J. 24, 1925–1934.
60. Backus, K.H., Kettenmann, H., and Schachner, M. (1988). Effect of benzodiazepines and pentobarbital on the GABA-induced depolarization in cultured astrocytes. Glia 1, 132–140.
61. Takamiya, Y., Kohsaka, S., Toya, S., Otani, M., and Tsukada, Y. (1988). Immunohistochemical studies on the proliferation of reactive astrocytes and the expression of cytoskeletal proteins following brain injury in rats. Brain Res. 466, 201–210.
62. van Praag, H., Kempermann, G., and Gage, F.H. (1999). Running increases cell proliferation and neurogenesis in the adult mouse dentate gyrus. Nat. Neurosci. 2, 266–270.
63. Kelly, K.M., Miller, E.R., Lepsveridze, E., Kharlamov, E.A., and McHedlishvili, Z. (2015). Posttraumatic seizures and epilepsy in adult rats after controlled cortical impact. Epilepsy Res. 117, 104–116.
64. Arndt, D.H., Lerner, J.T., Matsumoto, J.H., Madikians, A., Yudovin, S., Valino, H., McArthur, D.L., Wu, J.Y., Leung, M., Buxey, F., Szeliga, C., Van Hirtum-Das, M., Sankar, R., Brooks-Kayal, A., and Giza, C.C. (2013). Subclinical early posttraumatic seizures detected by continuous EEG monitoring in a consecutive pediatric cohort. Epilepsia 54, 1780–1788.
65. Parent, J.M., Yu, T.W., Leibowitz, R.T., Geschwind, D.H., Sloviter, R.S., and Lowenstein, D.H. (1997). Dentate granule cell neurogenesis is increased by seizures and contributes to aberrant network reorganization in the adult rat hippocampus. J. Neurosci. 17, 3727–3738.
66. Gould, E., Beylin, A., Tanapat, P., Reeves, A., and Shors, T.J. (1999). Learning enhances adult neurogenesis in the hippocampal formation. Nat. Neurosci. 2, 260–265.
67. Wang, Y., Hameed, M.Q., Rakhade, S.N., Iglesias, A.H., Muller, P.A., Mou, D.L., and Rotenberg, A. (2014). Hippocampal immediate early gene transcription in the rat fluid percussion traumatic brain injury model. Neuroreport 25, 954–959.
68. Abrous, D.N., Rodriguez, J., le Moal, M., Moser, P.C., and Barneoud, P. (1999). Effects of mild traumatic brain injury on immunoreactivity for the inducible transcription factors c-Fos, c-Jun, JunB, and Krox-24 in cerebral regions associated with conditioned fear responding. Brain Res. 826, 181–192.
69. Hernandez, T.D. (2006). Post-traumatic neural depression and neurobehavioral recovery after brain injury. J. Neurotrauma 23, 1211–1221.
70. van Praag, H., Kempermann, G., and Gage, F.H. (2000). Neural consequences of environmental enrichment. Nat. Rev. Neurosci. 1, 191–198.
71. Bruel-Jungerman, E., Davis, S., Rampon, C., and Laroche, S. (2006). Long-term potentiation enhances neurogenesis in the adult dentate gyrus. J. Neurosci. 26, 5888–5893.
72. Deisseroth, K., Singla, S., Toda, H., Monje, M., Palmer, T.D., and Malenka, R.C. (2004). Excitation-neurogenesis coupling in adult neural stem/progenitor cells. Neuron 42, 535–552.
73. Kitamura, T., Saitoh, Y., Murayama, A., Sugiyama, H., and Inokuchi, K. (2010). LTP induction within a narrow critical period of immature stages enhances the survival of newly generated neurons in the adult rat dentate gyrus. Mol. Brain 3, 13.
74. Nilsson, P., Ronne-Engstrom, E., Flink, R., Ungerstedt, U., Carlson, H., and Hillered, L. (1994). Epileptic seizure activity in the acute phase following cortical impact trauma in rat. Brain Res. 637, 227–232.
75. Gastaut, H., Naquet, R., Poire, R., and Tassinari, C.A. (1965). Treatment of status epilepticus with diazepam (Valium). Epilepsia 6, 167–182.
76. Hsieh, J., and Eisch, A.J. (2010). Epigenetics, hippocampal neurogenesis, and neuropsychiatric disorders: unraveling the genome to understand the mind. Neurobiol. Dis. 39, 73–84.
77. Butovsky, O., Ziv, Y., Schwartz, A., Landa, G., Talpalar, A.E., Pluchino, S., Martino, G., and Schwartz, M. (2006). Microglia activated by IL-4 or IFN-gamma differentially induce neurogenesis and oligodendrogenesis from adult stem/progenitor cells. Mol. Cell Neurosci. 31, 149–160.
78. Bye, N., Carron, S., Han, X., Agyapomaa, D., Ng, S.Y., Yan, E., Rosenfeld, J.V., and Morganti-Kossmann, M.C. (2011). Neurogenesis and glial proliferation are stimulated following diffuse traumatic brain injury in adult rats. J. Neurosci. Res. 89, 986–1000.
79. Carlson, S.W., Madathil, S.K., Sama, D.M., Gao, X., Chen, J., and Saatman, K.E. (2014). Conditional overexpression of insulin-like growth factor-1 enhances hippocampal neurogenesis and restores immature neuron dendritic processes after traumatic brain injury. J. Neuropathol. Exp. Neurol. 73, 734–746.
80. Jin, K., Zhu, Y., Sun, Y., Mao, X.O., Xie, L., and Greenberg, D.A. (2002). Vascular endothelial growth factor (VEGF) stimulates neurogenesis in vitro and in vivo. Proc. Natl. Acad. Sci. U S A 99, 11946–11950.
81. Larson, T.A., Thatra, N.M., Lee, B.H., and Brenowitz, E.A. (2014). Reactive neurogenesis in response to naturally occurring apoptosis in an adult brain. J. Neurosci. 34, 13066–13076.
82. Sierra, A., Encinas, J.M., Deudero, J.J., Chancey, J.H., Enikolopov, G., Overstreet-Wadiche, L.S., Tsirka, S.E., and Maletic-Savatic, M. (2010). Microglia shape adult hippocampal neurogenesis through apoptosis-coupled phagocytosis. Cell Stem Cell 7, 483–495.
83. Chatzi, C., Schnell, E., and Westbrook, G.L. (2015). Localized hypoxia within the subgranular zone determines the early survival of newborn hippocampal granule cells. Elife 4, e08722.
84. Esposito, M.S., Piatti, V.C., Laplagne, D.A., Morgenstern, N.A., Ferrari, C.C., Pitossi, F.J., and Schinder, A.F. (2005). Neuronal differentiation in the adult hippocampus recapitulates embryonic development. J. Neurosci. 25, 10074–10086.
85. Wu, X., and Castren, E. (2009). Co-treatment with diazepam prevents the effects of fluoxetine on the proliferation and survival of hippocampal dentate granule cells. Biol. Psychiatry 66, 5–8.
86. Stefovska, V.G., Uckermann, O., Czuczwar, M., Smitka, M., Czuczwar, P., Kis, J., Kaindl, A.M., Turski, L., Turski, W.A., and Ikonomidou, C. (2008). Sedative and anticonvulsant drugs suppress postnatal neurogenesis. Ann. Neurol. 64, 434–445.
87. Nochi, R., Kaneko, J., Okada, N., Terazono, Y., Matani, A., and Hisatsune, T. (2013). Diazepam treatment blocks the elevation of hippocampal activity and the accelerated proliferation of hippocampal neural stem cells after focal cerebral ischemia in mice. J. Neurosci. Res. 91, 1429–1439.
88. Bourin, M., Hascoet, M., Mansouri, B., Colombel, M.C., and Bradwejn, J. (1992). Comparison of behavioral effects after single and repeated administrations of four benzodiazepines in three mice behavioral models. J. Psychiatry Neurosci. 17, 72–77.
89. Arnot, M.I., Davies, M., Martin, I.L., and Bateson, A.N. (2001). GABA(A) receptor gene expression in rat cortex: differential effects of two chronic diazepam treatment regimes. J. Neurosci. Res. 64, 617–625.
90. Richter, L., de Graaf, C., Sieghart, W., Varagic, Z., Morzinger, M., de Esch, I.J., Ecker, G.F., and Ernst, M. (2012). Diazepam-bound GABAA receptor models identify new benzodiazepine binding-site ligands. Nat. Chem. Biol. 8, 455–464.

91. Thal, S.C., Timaru-Kast, R., Wilde, F., Merk, P., Johnson, F., Frauenknecht, K., Sebastiani, A., Sommer, C., Staib-Lasarzik, I., Werner, C., and Engelhard, K. (2014). Propofol impairs neurogenesis and neurologic recovery and increases mortality rate in adult rats after traumatic brain injury. Crit. Care Med. 42, 129–141.
92. Sierra, A., Martin-Suarez, S., Valcarcel-Martin, R., Pascual-Brazo, J., Aelvoet, S.A., Abiega, O., Deudero, J.J., Brewster, A.L., Bernales, I., Anderson, A.E., Baekelandt, V., Maletic-Savatic, M., and Encinas, J.M. (2015). Neuronal hyperactivity accelerates depletion of neural stem cells and impairs hippocampal neurogenesis. Cell Stem Cell 16, 488–503.
93. Blaiss, C.A., Yu, T.S., Zhang, G., Chen, J., Dimchev, G., Parada, L.F., Powell, C.M., and Kernie, S.G. (2011). Temporally specified genetic ablation of neurogenesis impairs cognitive recovery after traumatic brain injury. J. Neurosci. 31, 4906–4916.
94. Sun, D., Daniels, T.E., Rofle, A., Waters, M., and Hamm, R.J. (2015). Inhibition of injury-induced cell proliferation in the dentate gyrus of the hippocampus impairs spontaneous cognitive recovery following traumatic brain injury. J. Neurotrauma 32, 495–505.
95. Deng, W., Saxe, M.D., Gallina, I.S., and Gage, F.H. (2009). Adult-born hippocampal dentate granule cells undergoing maturation modulate learning and memory in the brain. J. Neurosci. 29, 13532–13542.
96. Dupret, D., Revest, J.M., Koehl, M., Ichas, F., De Giorgi, F., Costet, P., Abrous, D.N., and Piazza, P.V. (2008). Spatial relational memory requires hippocampal adult neurogenesis. PLoS One 3, e1959.
97. Raber, J., Rola, R., LeFevour, A., Morhardt, D., Curley, J., Mizumatsu, S., VandenBerg, S.R., and Fike, J.R. (2004). Radiation-induced cognitive impairments are associated with changes in indicators of hippocampal neurogenesis. Radiat. Res. 162, 39–47.
98. Kleindienst, A., McGinn, M.J., Harvey, H.B., Colello, R.J., Hamm, R.J., and Bullock, M.R. (2005). Enhanced hippocampal neurogenesis by intraventricular S100B infusion is associated with improved cognitive recovery after traumatic brain injury. J. Neurotrauma 22, 645–655.
99. Wu, H., Lu, D., Jiang, H., Xiong, Y., Qu, C., Li, B., Mahmood, A., Zhou, D., and Chopp, M. (2008). Simvastatin-mediated upregulation of VEGF and BDNF, activation of the PI3K/Akt pathway, and increase of neurogenesis are associated with therapeutic improvement after traumatic brain injury. J. Neurotrauma 25, 130–139.
100. Sun, D., Bullock, M.R., McGinn, M.J., Zhou, Z., Altememi, N., Hagood, S., Hamm, R., and Colello, R.J. (2009). Basic fibroblast growth factor-enhanced neurogenesis contributes to cognitive recovery in rats following traumatic brain injury. Exp. Neurol. 216, 56–65.
101. Leal, G., Afonso, P.M., Salazar, I.L., and Duarte, C.B. (2015). Regulation of hippocampal synaptic plasticity by BDNF. Brain Res. 1621, 82–101.
102. Knoth, R., Singec, I., Ditter, M., Pantazis, G., Capetian, P., Meyer, R.P., Horvat, V., Volk, B., and Kempermann, G. (2010). Murine features of neurogenesis in the human hippocampus across the lifespan from 0 to 100 years. PLoS One 5, e8809.
103. Spalding, K.L., Bergmann, O., Alkass, K., Bernard, S., Salehpour, M., Huttner, H.B., Bostrom, E., Westerlund, I., Vial, C., Buchholz, B.A., Possnert, G., Mash, D.C., Druid, H., and Frisen, J. (2013). Dynamics of hippocampal neurogenesis in adult humans. Cell 153, 1219–1227.
104. Boldrini, M., Fulmore, C.A., Tartt, A.N., Simeon, L.R., Pavlova, I., Poposka, V., Rosoklija, G.B., Stankov, A., Arango, V., Dwork, A.J., Hen, R., and Mann, J.J. (2018). Human hippocampal neurogenesis persists throughout aging. Cell Stem Cell 22, 589–599.e5.
105. Taylor, S.R., Smith, C., Harris, B.T., Costine, B.A., and Duhaime, A.C. (2013). Maturation-dependent response of neurogenesis after traumatic brain injury in children. J. Neurosurg. Pediatr. 12, 545–554.
106. Yu, T.S., Zhang, G., Liebl, D.J., and Kernie, S.G. (2008). Traumatic brain injury-induced hippocampal neurogenesis requires activation of early nestin-expressing progenitors. J. Neurosci. 28, 12901–12912.
107. Ho, N.F., Hooker, J.M., Sahay, A., Holt, D.J., and Roffman, J.L. (2013). In vivo imaging of adult human hippocampal neurogenesis: progress, pitfalls and promise. Mol. Psychiatry 18, 404–416.

Address correspondence to:
Eric Schnell, MD, PhD
VA Portland Health Care System, P3ANES
3710 S.W. U.S. Veterans Hospital Road
Portland, OR 97239

E-mail: schneler@ohsu.edu

Early detonation by sprouted mossy fibers enables aberrant dentate network activity

William D. Hendricks[a,b], Gary L. Westbrook[c], and Eric Schnell[b,d,1]

[a]Neuroscience Graduate Program, Vollum Institute, Oregon Health & Science University, Portland, OR 97239; [b]Department of Anesthesiology and Perioperative Medicine; Oregon Health & Science University, Portland, OR 97239; [c]Vollum Institute, Oregon Health & Science University, Portland, OR 97239; and [d]Veterans Affairs Portland Health Care System, Portland, OR 97239

Edited by Roger A. Nicoll, University of California, San Francisco, CA, and approved April 16, 2019 (received for review December 13, 2018)

In temporal lobe epilepsy, sprouting of hippocampal mossy fiber axons onto dentate granule cell dendrites creates a recurrent excitatory network. However, unlike mossy fibers projecting to CA3, sprouted mossy fiber synapses depress upon repetitive activation. Thus, despite their proximal location, relatively large presynaptic terminals, and ability to excite target neurons, the impact of sprouted mossy fiber synapses on hippocampal hyperexcitability is unclear. We find that despite their short-term depression, single episodes of sprouted mossy fiber activation in hippocampal slices initiated bursts of recurrent polysynaptic excitation. Consistent with a contribution to network hyperexcitability, optogenetic activation of sprouted mossy fibers reliably triggered action potential firing in postsynaptic dentate granule cells after single light pulses. This pattern resulted in a shift in network recruitment dynamics to an "early detonation" mode and an increased probability of release compared with mossy fiber synapses in CA3. A lack of tonic adenosine-mediated inhibition contributed to the higher probability of glutamate release, thus facilitating reverberant circuit activity.

epilepsy | mossy fiber | sprouting | seizure | adenosine

Mossy fibers contacting CA3 pyramidal cells have a low probability of release (P_r) but show profound short-term facilitation (1). These "conditional detonator" synapses strongly drive postsynaptic cell firing during repetitive activation (2). In experimental and human epilepsy, mossy fiber axons sprout collaterals onto the proximal dendrites of other dentate granule cells (3–6), where conditional detonation could be highly epileptogenic. However, sprouted mossy fibers are smaller than mossy fiber synapses in CA3 (7–9) and rapidly depress during repetitive activation (8), suggesting the extent with which they drive seizure activity could be limited (10).

Despite multiple lines of evidence demonstrating de novo recurrent connections in rodent models of epilepsy, the impact of mossy fiber sprouting on circuit dynamics remains uncertain (11–14). Sprouted mossy fibers are absent under nonpathological conditions, and the formation of novel recurrent connections capable of activating postsynaptic granule cells (15) could induce runaway excitation, particularly if they robustly activate the typically quiescent dentate network. Although increased dentate excitation occurs in temporal lobe epilepsy (16, 17), the challenge of isolating and selectively stimulating sprouted mossy fibers has severely hampered studies that directly examine sprouted mossy fiber synapses (15) and an understanding of how the activation of these fibers might contribute to epileptiform activity.

Here, we selectively activated sprouted mossy fiber axons with optogenetics to determine their influence on postsynaptic granule cell firing and dentate gyrus activity. We find that sprouted mossy fibers reliably drive postsynaptic action potential (AP) firing in dentate granule cells and initiate recurrent circuit activity even in the absence of manipulations to increase excitability. This effect is mediated by increased release probability at these synapses, attributed to a lack of tonic adenosine signaling in the inner molecular layer of the dentate gyrus. The increased P_r allows sprouted mossy fiber activation to reliably recruit postsynaptic circuits, as primed network "spark plugs."

Results

As the functional contribution of mossy fiber sprouting to epileptogenesis remains controversial (10–13), we combined the pilocarpine model of temporal lobe epilepsy with electrophysiology to directly examine the contribution of sprouted mossy fiber activation to epileptiform activity, as this model reliably induces dense mossy fiber sprouting (see *Methods*, also see ref. 8). To isolate sprouted mossy fibers from other granule cell inputs, we used DcxCre::ChR2 mice (18) to selectively label neonatally born granule cells with channelrhodopsin2 (ChR2) (Fig. 1*A*). We then prepared acute mouse hippocampal slices and optogenetically activated sprouted mossy fibers while recording from ChR2-negative (unlabeled) granule cells (Fig. 1 *B* and *C* and *SI Appendix*, Fig. S1; also see ref. 8). Optogenetic activation of sprouted mossy fibers evoked EPSCs in dentate granule cells only in slices from pilocarpine-treated mice (Fig. 1 *D* and *E*; also see ref. 8). Postsynaptic cells, filled with Alexa Fluor 568 dye during recordings, did not have hilar basal dendrites (0 of 32 cells; Fig. 1*C*), indicating that LED-evoked responses originated from recurrent (sprouted mossy fiber) synaptic inputs.

In addition to monosynaptic sprouted mossy fiber–granule cell (smf-GC) EPSCs, we frequently observed LED-evoked epileptiform activity following single light pulses (Fig. 1*D*, *Right*). Responses identified as bursts had, on average, 2.3 ± 0.3 EPSCs during a burst (n = 13 cells). These bursts were not a result of altered intrinsic properties compared with cells with single or no evoked recurrent EPSCs (R_i, input resistance: cells without bursts, 610 ± 47 MΩ, n = 19 cells; cells with bursts, 527 ± 77 MΩ, n = 13 cells; unpaired t test, t_{30} = 0.9711, P = 0.3392; C_m, cell

Significance

Sprouted mossy fibers are one of the hallmark histopathological findings in experimental and human temporal lobe epilepsy. These fibers form recurrent excitatory synapses onto other dentate granule cells that display profound short-term depression. Here, however, we show that although these sprouted mossy fibers weaken substantially during repetitive activation, their initial high probability of glutamate release can activate reverberant network activity. Furthermore, we find that a lack of tonic adenosine inhibition enables this high probability of release and, consequently, recurrent network activity.

Author contributions: W.D.H., G.L.W., and E.S. designed research; W.D.H. performed research; W.D.H. analyzed data; and W.D.H. and E.S. wrote the paper.

The authors declare no conflict of interest.

This article is a PNAS Direct Submission.

[1]To whom correspondence should be addressed. Email: schneler@ohsu.edu.

This article contains supporting information online at www.pnas.org/lookup/suppl/doi:10.1073/pnas.1821227116/-/DCSupplemental.

Published online May 13, 2019.

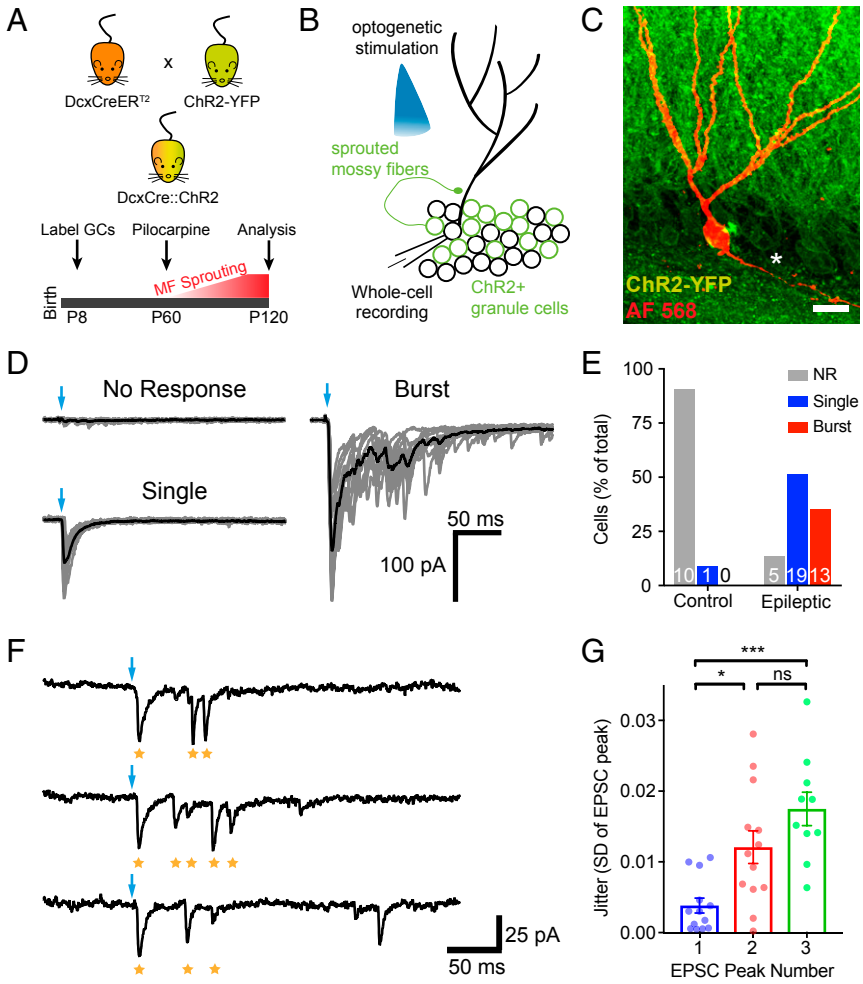

Fig. 1. Stimulation of sprouted mossy fibers triggers spiking in postsynaptic dentate granule cells and recurrent network activity. (*A*) Experimental design for granule cell labeling and induction of epileptic mossy fiber sprouting. DcxCreER^{T2} mice were bred with conditional ChR2-YFP (Ai32) reporter mice (*Upper*) and given TAM at P8 to turn on reporter gene expression (*Lower*). At 2 mo old (P60), mice were given pilocarpine to induce seizures and mossy fiber sprouting or kept as controls. All analysis was at P120. (*B*) Whole-cell recordings were performed on ChR2-negative dentate granule cells (black circles) and sprouted mossy fiber axons were stimulated with blue (470 nm) LED light delivered through the objective. (*C*) Representative confocal image of a recorded granule cell filled with Alexa Fluor 568 (50 μM) during whole-cell recording (levels and gamma adjusted for clarity). Asterisk designates mossy fiber axon; no basal dendrites were present. (Scale bar: 10 μm.) (*D*) Example traces from cells with no response (*Upper Left*), single EPSCs (*Lower Left*), and epileptiform bursts (*Right*) after single optogenetic stimulation of ChR2^{+} granule cells (blue arrows). Scale bar at *Right* applies to all traces. (*E*) Frequency of cells with no response (NR), single EPSCs (Single), and EPSC bursts (Burst) in control and epileptic mice. Number of cells in each category are listed on the graph. (*F*) Three consecutive traces taken from a cell with EPSC bursts. Optogenetic stimulation (blue arrow) evoked an initial EPSC (likely monosynaptic) followed by variably timed burst EPSCs. Gold stars designate detected EPSCs. EPSCs occurring later in the sweep were not counted, as they did not occur within our 100-ms poststimulus timeframe to be considered part of the burst. (*G*) Jitter (trial to trial variability of EPSC onsets, as SD) taken from the first three peaks in an EPSC burst is increased after the first EPSC peak (EPSC jitter: Peak 1, $n = 13$; Peak 2, $n = 13$; Peak 3, $n = 10$; one-way ANOVA, $F_{2,33} = 12.0$, $P = 0.0001$; Tukey's test, Peak 1 vs. Peak 2, $P = 0.0105$; Peak 1 vs. Peak 3, $P < 0.0001$; Peak 2 vs. Peak 3, $P = 0.1544$). High variability in second and third EPSC peaks within a burst suggest that they result from polysynaptic activity. Summary data presented as mean ± SEM. *$P < 0.05$; ***$P < 0.001$; ns, not significant.

capacitance: cells without bursts, 51.5 ± 3.8 pF, $n = 19$ cells; cells with bursts, 46.8 ± 3.8, $n = 13$ cells; unpaired t test, $t_{30} = 0.8302$, $P = 0.4130$). Optogenetic stimulation only elicited single spikes in ChR2-expressing granule cells (number of APs per 1 ms of light pulse: 0.98 ± 0.09, $n = 5$ cells), indicating that sprouted mossy fiber activation initiated recurrent activity. Consistent with polysynaptic activation, EPSC peaks during bursts (EPSC peaks 2–3) had high jitter (Fig. 1 *F* and *G*). One possible source of these bursts is through the activation of additional populations of granule cells with their own sprouted mossy fibers, if sprouted mossy fibers could effectively drive postsynaptic firing.

Unlike healthy mossy fiber–CA3 synapses (1) that are described as conditional detonators, sprouted mossy fiber synapses exhibit profound frequency-dependent short-term depression (*SI Appendix*, Fig. S2, see also ref. 8), which may limit their ability to drive postsynaptic firing (10). Thus, we compared patterns of synaptically evoked spike generation in postsynaptic target cells at these two different synapses using a short 10-Hz train of optogenetic stimulation. In striking contrast to synaptic facilitation and delayed CA3 pyramidal cell spike generation at mf-CA3 synapses, 10-Hz stimulation of sprouted mossy fiber synapses induced postsynaptic spikes only at the beginning of the train (Fig. 2). Importantly, this firing pattern did not result from a failure to activate sprouted mossy fibers in epileptic brains, as these fibers maintain AP fidelity throughout optogenetic trains (*SI Appendix*, Fig. S1). Thus, the failure to maintain postsynaptic activation resulted instead from reduced glutamate release later in the train, consistent with short-term synaptic depression at

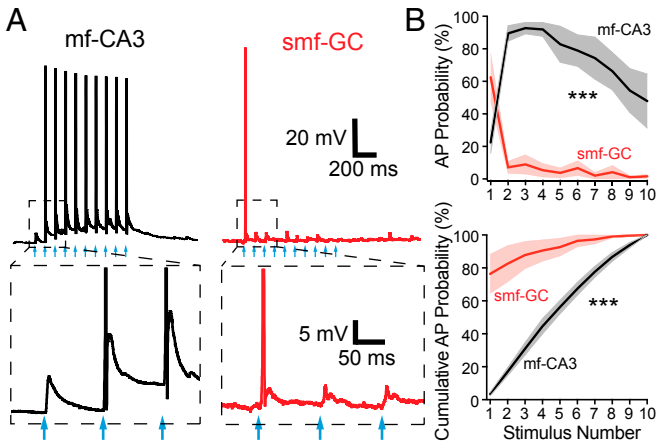

Fig. 2. Sprouted mossy fiber activation drives postsynaptic granule cell firing early during brief trains. (*A*) Representative current clamp recordings during mf-CA3 (black trace) and smf-GC (red trace) activation by 10-Hz, 10-pulse LED trains (blue arrows). Dashed boxes represent insets (below) highlighting facilitation of mf-CA3 EPSPs (*Left*) and depression of smf-GC EPSPs (*Right*). (*B*) AP probability (*Upper*) is shifted to the first stimulus after smf-GC activation relative to mf-CA3 activation (mf-CA3, $n = 6$ cells; smf-GC, $n = 8$ cells, two-way RM ANOVA, $F_{1,12} = 85.68$, $P < 0.0001$; Sidak's multiple comparisons test, Stimulus 1, $P = 0.0048$, Stimuli 2–9, all $P < 0.0001$, Stimulus 10, $P = 0.0006$). Cumulative AP distribution (*Lower*) was also significantly shifted (Kolmogorov–Smirnov test, $P = 0.0006$). Summary data presented as mean ± SEM ***$P < 0.001$.

these synapses (8). Despite this depression, however, single pulses triggered circuit activation sufficient to recruit additional recurrent networks (Fig. 1*D*).

Both the frequency-dependent short-term depression and the robust initial recruitment of postsynaptic cell firing during recurrent activation (Fig. 2*B*) could result from a high initial P_r at sprouted mossy fiber synapses. To directly test for increased P_r, we measured use-dependent MK-801 block kinetics during activation of both types of mossy fiber synapses. Optogenetically evoked NMDAR-mediated synaptic currents were isolated by voltage-clamping granule cells to −70 mV in Mg^{2+}-free ACSF, in the presence of NBQX (10 μM) and SR95531 (10 μM) to block AMPA and $GABA_A$ receptors, respectively. After baseline EPSC recording, LED stimulation was paused for 10 min while MK-801 (40 μM) was washed onto the slice and allowed to equilibrate. Upon resuming LED stimulation (0.05 Hz), MK-801 progressively blocked NMDAR-EPSCs from smf-GC and mf-CA3 synapses (Fig. 3*A*). The rate of block was faster for sprouted mossy fiber synapses (Fig. 3*B*), indicating a higher P_r. Interestingly, MK-801 block rate at smf-GC synapses was better fit by a double-exponential decay model (Fig. 3*C*), whereas at mf-CA3 synapses, a single exponential model was sufficient, suggesting increased synaptic heterogeneity at sprouted mossy fiber synapses (19). Overall, the increased P_r at sprouted mossy fiber synapses likely contributes to target granule cell firing and, therefore, the spread of recurrent excitation in epileptic brains.

Extracellular adenosine inhibits neurotransmitter release at mossy fiber synapses in CA3 via A1-type adenosine receptors (A_1Rs) located on mossy fiber terminals. This tonic activation of presynaptic A_1Rs contributes to the profound short-term plasticity at these synapses (20, 21). As altered adenosine metabolism may be a contributing factor in epileptogenesis (22–24), we posited that sprouted mossy fibers might manifest an increased P_r due to a reduction in A_1R-mediated inhibition. To measure tonic A_1R-mediated inhibition of sprouted mossy fibers in epileptic mice, we washed on the selective high-affinity A_1R antagonist, 8-Cyclopentyl-1,3-dipropylxanthine (DPCPX, 200 nM), while recording sprouted mossy fiber-mediated responses. In contrast to the enhancement of synaptic transmission at healthy mf-CA3 synapses (Fig. 4 *A* and *B*, also see ref. 20), DPCPX had no effect on sprouted mossy fiber EPSCs (Fig. 4 *A* and *B*), indicating a lack of tonic A_1R signaling. The DPCPX-induced increase in EPSC amplitudes at mf-CA3 synapses coincided with decreased PPR (paired-pulse ratio, P_2/P_1: pre-DPCPX, 2.36 ± 0.37; post-DPCPX, 1.37 ± 0.12, $n = 6$ cells; paired t test, $t_5 = 3.408$ $P = 0.0191$), as expected for a presynaptic effect on A_1Rs.

To determine whether the lack of tonic A_1R-mediated inhibition at sprouted mossy fiber synapses resulted from an absence of presynaptic adenosine receptors, we washed on the selective A_1R agonist, 2-Chloro-N^6-cyclopentyladenosine (CCPA, 1 μM). CCPA reduced sprouted mossy fiber EPSCs (Fig. 4 *C* and *D*) and increased paired-pulse facilitation (*SI Appendix*, Fig. S3). Thus, A_1Rs were present and functional on sprouted mossy fiber terminals, indicating that the lack of tonic A_1R modulation was due to a reduced extracellular adenosine concentration. CCPA decreased the probability of release at sprouted mossy fiber synapses, but it did not restore frequency facilitation (*SI Appendix*, Fig. S4), suggesting that the molecular mechanisms underlying synaptic facilitation at mossy fiber terminals cannot be restored solely by increasing A_1R activation.

Finally, to test whether reduced A_1R activation and increased P_r at sprouted mossy fiber synapses contributes to recurrent circuit activation, we examined the effect of A_1R activation using hippocampal slices from epileptic mice. When applied to slices demonstrating EPSC bursts after sprouted mossy fiber activation, the A_1R agonist CCPA reduced recurrent EPSCs (Fig. 4 *E* and *F*) as well as the charge transfer carried by polysynaptic bursts (% of total charge transfer carried by burst: pre-CCPA, 36.5 ± 5.1%, post-CCPA 22.8 ± 4.4%, $n = 5$ cells, paired t test, $t_4 = 3.497$, $P = 0.0250$). Together, these data indicate that

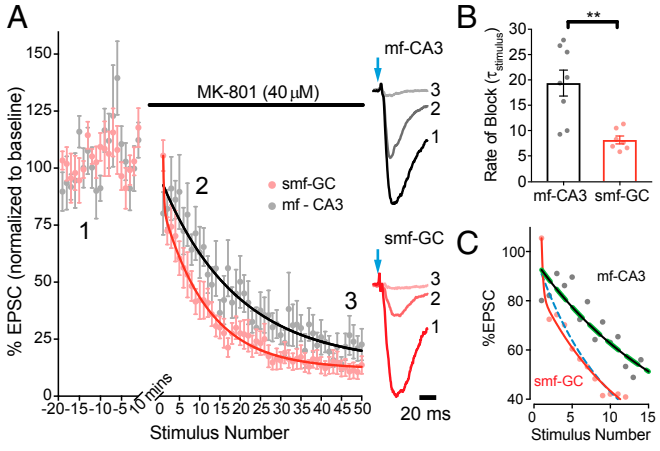

Fig. 3. Elevated probability of release at sprouted mossy fiber synapses. (*A*) P_r was measured from the kinetics of use-dependent MK-801 block of NMDAR-mediated EPSCs during 0.05-Hz LED stimulation. Averaged and normalized responses (*Left*) are plotted before and after bath application of MK-801 (40 μM; mf-CA3, $n = 8$; smf-GC, $n = 7$). Representative, peak-scaled NMDAR EPSC averages (*Right*) were taken during baseline, shortly after resuming LED stimulation, and at the end of the experiment, numbered 1, 2, 3, respectively. (*B*) Average rate of MK-801 block measured in individual cells. MK-801 rate of block was significantly faster at sprouted mossy fiber synapses (unpaired t test, $t_{13} = 3.942$, $P = 0.0017$), indicating higher P_r. (*C*) Same as in *A*, but only showing the first 15 sweeps in MK-801. Single (solid lines) and double (dashed lines) exponential fits are plotted for smf-GC (red and blue) and mf-CA3 (black and green). Sprouted mossy fibers are better fit by double exponential decays (extra sum of squares F test, $F_{2,395} = 5.07$, $P = 0.0067$), whereas mf-CA3 synapses are fit identically by single and double models. All data are presented as mean ± SEM. **$P < 0.01$.

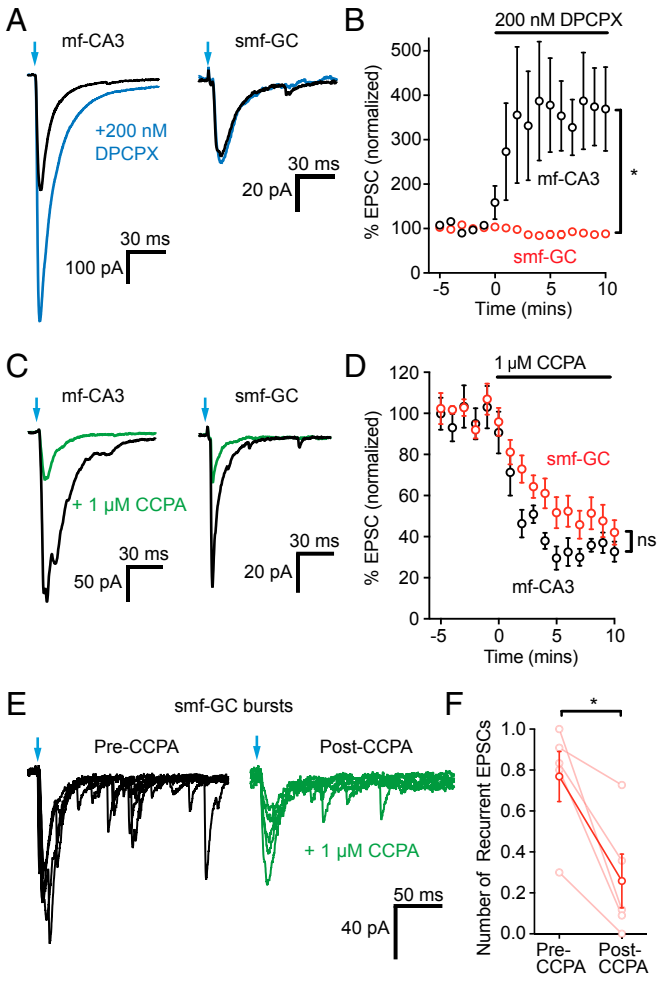

Fig. 4. Lack of tonic adenosine contributes to increased release probability and polysynaptic activity. (*A*) mf-CA3 (*Left*) and smf-GC (*Right*) EPSCs before (black traces) and after (blue traces) washing on the adenosine 1a receptor (A_1R) antagonist DPCPX (200 nM). Bath application of DPCPX facilitates mf-CA3 EPSCs ($n = 8$ cells, paired t test, $t_7 = 5.77$, $P = 0.0007$) but has no effect on EPSC amplitudes at smf-GC synapses ($n = 5$ cells, paired t test, $t_4 = 1.39$, $P = 0.2364$). (*B*) Normalized EPSC amplitudes of mf-CA3 (black, $n = 8$ cells) and smf-GC (red, $n = 5$ cells) responses before and during DPCPX administration (unpaired t test, $t_{11} = 3.63$ $P = 0.0040$). (*C*) The A_1R agonist CCPA (1 μM) inhibits both mf-CA3 (*Left*) and smf-GC (*Right*) EPSCs similarly (baseline, black example traces; CCPA, green traces). (*D*) Normalized mf-CA3 (black) and smf-GC (red) EPSC amplitudes during CCPA application, demonstrating intact A_1R responses at both synapses (mf-CA3, $n = 7$ cells, smf-GC, $n = 12$ cells; unpaired t test, $t_{17} = 1.08$, $P = 0.2954$). (*E*) Adenosine A_1R agonism inhibits recurrent polysynaptic network activity evoked by single-pulse optogenetic stimulation of sprouted mossy fibers. Examples are five consecutive EPSC traces overlaid from the same cell, pre- and post-CCPA (black and green, respectively). (*F*) Quantification of EPSC burst inhibition by CCPA at smf-GC synapses. CCPA (1 μM) reduces the mean number of recurrent EPSCs during a burst (number of recurrent EPSCs per epoch, $n = 5$ cells, $t_4 = 3.963$, $P = 0.0166$). Summary data presented as mean ± SEM. *$P < 0.05$; ns, not significant.

reduced A_1R activation at granule cell outputs contributes to hyperexcitability in the dentate gyrus in epileptic brains.

Discussion

Here, we show that sprouted mossy fibers can trigger reverberating network activity despite their profound short-term depression. This recurrent network activation is enabled by a high probability of release, resulting in early detonation of postsynaptic cells. Moreover, this is due, at least in part, to the lack of tonic adenosine inhibition at sprouted mossy fiber synapses in the inner molecular layer.

The retrograde sprouting of mossy fibers is common to both animal models of epilepsy and human patients with temporal lobe epilepsy (25), yet the functional impact of these recurrent synapses is not well understood (10, 11). We demonstrate that single optogenetic stimulation of these fibers can produce bursts of recurrent EPSCs, suggesting that sprouted mossy fibers effectively recruit the local network. This observation is consistent with paired granule cell recordings from epileptic mice (15), which suggest that sprouted mossy fibers form recurrent excitatory connections capable of driving postsynaptic cell spiking. Critically, we find that sprouted mossy fibers can potently trigger granule cell AP firing with single coordinated release events, which could lead to bursts as successive rounds of sprouted mossy fibers are activated through additional granule cell firing.

The functional effects of sprouted mossy fibers on dentate excitability in ex vivo slice preparations has been difficult to determine, as it sometimes requires modulation of the extracellular environment to reduce the masking effects of inhibition (16, 26–29). This suggests that although the state of the epileptic dentate network may be relatively stable (30), subtle changes in external K^+ concentration (27, 28), inhibition (16, 28), or adenosine (23, 31, 32) could shift the network to a more unstable, hyperexcitable state, during which sprouted mossy fibers can readily trigger epileptiform activity. The absence of tonic adenosine signaling appears to be intrinsic to epileptic slices, recorded using standard solutions. However, it remains likely that changes in adenosine-mediated signaling may serve as another conditional factor in vivo, which might vary over time and contribute to the occurrence (or avoidance) of seizure activity, given the presence of functional adenosine receptors at these synapses.

All EPSC bursts were self-limited, which may be a manifestation of the strong short-term depression of the smf-GC synapse (8, 15). This also helps explain prior indirect observations made using extracellular retrograde stimulation of mossy fibers, which caused self-limited episodes of granule cell population spiking in slices from epileptic rats (33). By using direct optogenetic stimulation of sprouted fibers, we demonstrate sprouted mossy fibers can indeed drive granule cell firing even with inhibition intact and low (3 mM) external K^+ concentrations. We recognize that the conclusions that can be made while using optogenetic stimulation in an acute slice preparation in regards to seizure activity in vivo are limited, primarily due to the isolation of slices from other brain networks and the cerebral extracellular environment and synchronized activation of sprouted terminals. However, our ability to robustly trigger recurrent network activation suggests that recurrent networks are widespread even within our 300-μm brain slices, and that recurrent interconnectivity might be even more extreme within the intact brain.

The increased P_r at sprouted mossy fibers provides a reasonable mechanism that could enable sprouted mossy fibers to act as spark plugs to hyperactivate local dentate gyrus networks. Our direct comparisons of P_r between smf-GC and mf-CA3 synapses are consistent with previous data demonstrating a larger success rate at individual smf-GC connections (0.35) (15) than the prior estimate of P_r at mf-CA3 synapses of 0.2–0.28 (34). We propose that the increased P_r at these sprouted synapses is, at least in part, due to reduced tonic inhibition by adenosine at the smf-GC synapse.

Although we did observe an increase in PPR with CCPA (suggesting that it lowered P_r), our observation that 1-Hz facilitation was not restored by adenosine agonism was somewhat surprising, given the extent to which A1R antagonism occludes frequency facilitation at mf-CA3 synapses in healthy brains (20). This indicates that tonic adenosine alone is unlikely to be the only mechanism controlling short-term plasticity in the smf-GC synapse. This is supported by the previous observation that

healthy mossy fiber synapses still express small but significant frequency-dependent facilitation even in the presence of A1R blockade or A1R gene knockout (20). Thus, the short-term depression remaining at smf-GC synapses even in the presence of CCPA could be due to other changes in neuromodulatory tone in the epileptic dentate gyrus or altered expression of specific components of the release machinery required for facilitation (35, 36). Even in healthy brains, the expression of frequency-dependent facilitation by mossy fibers is target-specific (37) and, thus, the remaining differences may also partly derive from differences in the postsynaptic complement between granule cells and CA3 pyramidal cells.

Does the lack of tonic adenosine in the dentate gyrus contribute to seizure activity in epilepsy? Although systemic or local injections of A_1R agonists can reduce the severity of seizures (31, 32), adenosine has broad inhibitory effects throughout the brain. Here, the absence of tonic adenosine signaling at these synapses heightens the excitability of dentate gyrus circuitry, which was reduced by pharmacological A_1R activation (Fig. 4). As the granule cell network is implicated in spontaneous seizures in vivo (38), restoration or augmentation of extracellular adenosine could reduce recurrent circuit dynamics in the dentate gyrus and provide one mechanism for the observed in vivo effects of adenosine (31, 32). Thus, although seizure activity in epileptic brains likely results from multiple hyperexcitable circuit elements, the lack of tonic adenosine signaling in the dentate gyrus shifts sprouted mossy fiber synapses from "conditional detonators" to "early detonators," which could contribute to the initiation of generalized seizures.

Methods

Animals. All experiments were carried out in accordance with local, state, and federal guidelines, and protocols were approved by Oregon Health & Science University (OHSU) and Veterans Affairs Institutional Animal Care and Use Committees. Housing was provided by OHSU's Department of Comparative Medicine vivarium accredited by the Association for Assessment and Accreditation of Laboratory Animals. To generate DcxCre::ChR2 mice, homozygous *doublecortin-CreER^{T2}* (line F18; RRID:MGI:5438982) mice were bred with homozygous *Gt(ROSA)26Sor$^{tm32(CAG-COP4*H134R/EYFP)Hze}$* (Ai32; RRID:IMSR_JAX:012569) and used as described (8, 18). Briefly, Cre-mediated combination was induced by tamoxifen (TAM) at postnatal day (P)8 (two injections, 12 h apart, 20 mg/kg in corn oil, i.p.), to permanently label neonatally generated granule cells with ChR2-eYFP in DcxCre::ChR2 heterozygous mice. Status epilepticus was induced in 2-mo-old male mice with pilocarpine (325 mg/kg i.p.; Cayman Chemicals) after pretreating with an i.p. injection of scopolamine methyl bromide (Sigma-Aldrich). Seizures were graded on the modified Racine Scale (39); status epilepticus (SE) was defined when a mouse had three or more Racine Grade 3 seizures, followed by continuous grade 2 seizing. Following 2 h of SE, seizures were terminated with diazepam (10 mg/kg i.p.; Hospira, Inc.) and given soft food and i.p. injections of 5% glucose in 0.45% normal saline to aid in recovery. Mice that did not develop SE were humanely killed by carbon dioxide inhalation and cervical dislocation and excluded from further analysis. These criteria reliably produce dense mossy fiber sprouting as measured by ZnT3 staining in the IML, and a high density of sprouted mossy fibers originating from granule cells specifically labeled at this timepoint (8). A total of 23 healthy control mice and 19 pilocarpine-treated mice were used in this study.

Slice Physiology. Acute brain slices for ex vivo electrophysiology were prepared as described (8). In brief, 4-mo-old male DcxCre::ChR2 mice were anesthetized with 4% isoflurane, followed by injection of 1.2% avertin (Sigma-Aldrich). Mice were transcardially perfused with 10 mL of ice-cold *N*-methyl-D-glucamine (NMDG)-based cutting solution, containing the following (in mM): 93 NMDG, 30 $NaHCO_3$, 24 glucose, 20 Hepes, 5 Na-ascorbate, 5 *N*-acetyl cysteine, 3 Na-pyruvate, 2.5 KCl, 2 thiourea, 1.2 NaH_2PO_4, 10 $MgSO_4$, and 0.5 $CaCl_2$. Mice were rapidly decapitated and 300-μm sagittal slices were prepared with a Leica VT1200S vibratome. This method was chosen to best preserve CA3 pyramidal cell health and mossy fiber axons from these 4-mo-old mice. For some dentate granule cell recordings, the hippocampus was dissected, and 300-μm transverse hippocampal sections were prepared in ice-cold NMDG solution, which allowed us to maximize the number of slices obtained from epileptic animals. We did not observe any physiological differences between the two preparations during granule cell recordings, including the frequency of smf-GC bursts, so these results were combined. Slices from both preparations recovered in warm NMDG cut solution for 15 min followed by standard ACSF at room temperature for 1 h before recording.

Dentate granule cell and CA3 pyramidal cell recordings were obtained with 3–5 MΩ borosilicate glass pipettes filled with internal solution. The Cs^+-based internal solution for voltage-clamp experiments contained the following (in mM): 113 Cs-gluconate, 17.5 CsCl, 10 Hepes, 10 EGTA, 8 NaCl, 2 Mg-ATP, 0.3 Na-GTP, 0.05 Alexa Fluor 568, pH adjusted to 7.3 with CsOH, with a final osmolarity of 295 mOsm; QX-314-Cl (5 mM; Tocris Bioscience) was included to block unclamped APs. The K^+-based internal solution for current-clamp experiments contained the following (in mM): 130 K-gluconate, 20 KCl, 10 Hepes, 4 Mg-ATP, 0.3 Na-GTP, 0.1 EGTA, 0.05 Alexa Fluor 568, pH adjusted to 7.2 KOH, with a final osmolarity of 295 mOsm. Granule cells and CA3 pyramidal cells were identified with infrared differential interference contrast microscopy on an Olympus BX-51WI microscope. Whole-cell recordings were obtained by making high-resistance seals (>5 GΩ) and applying brief suction. Cells were filled with Alexa Fluor 568 dye to visually confirm cell type and assess for presence of hilar basal dendrites. Series resistance was uncompensated, and cells with a >30% change in series resistance were excluded from analysis. Liquid junction potential was 8 mV and was uncorrected. For current-clamp recordings, minimal negative current was injected, if necessary, to maintain a resting potential of −70 mV in dentate granule cells and CA3 pyramidal cells.

Pulses of blue LED-powered (Thorlabs) light (1 ms, 470 nm, 8 mW/cm^2, 0.05 Hz) were delivered through a 40x water immersion objective, targeted at the stratum lucidum for CA3 recordings and inner molecular layer for granule cell recordings. Stimulation frequency was modified for various experiments as noted in the text. Signals were amplified with an AxoPatch 200B amplifier (Molecular Devices), low-pass Bessel-filtered at 5 kHz, and digitized and sampled at 10 kHz using a NIDAQ (National Instruments) analog-to-digital board. Data were captured using a custom Igor Pro 8 (Wavemetrics) script and NIDAQmx (National Instruments) plugins. For presentation of EPSCs, a 2-kHz Gaussian filter was applied, post hoc.

Statistical Analysis. Curve fitting and EPSC trace averaging was carried out in Igor Pro 8 (Wavemetrics) using built-in and custom functions, respectively. Epileptiform burst activity (multiple EPSCs to single stimulus) was determined by eye, aided by fitting a single exponential curve to the initial decay and identifying delayed EPSC peaks rising above the decay fit line. Peak detection was implemented in Igor Pro by identifying zero-point crossings of thresholded peaks on the first-order derivative of the EPSC. Charge transfer measurements were implemented with Igor Pro's area function. Additional statistical analysis was performed in Prism 8 (GraphPad). Normality was tested with the Shapiro–Wilk normality test before statistical test selection. Paired and unpaired *t* tests were used for normally distributed datasets; Mann–Whitney and Wilcoxon matched-pairs signed rank test were used for nonparametric datasets. For all experiments, significance was determined by $P < 0.05$ ($*P < 0.05$, $**P < 0.01$, $***P < 0.001$). All summary data are presented as mean ± SEM.

ACKNOWLEDGMENTS. We thank Drs. Zhi-Qi Xiong and Xuewen Cheng (Shanghai Institute for Neuroscience) for providing the DcxCreER^{T2} mouse line and members of the E.S. and G.L.W. laboratories for critical feedback and discussion on the manuscript. Research funding was provided by Department of Veterans Affairs, Veterans Health Administration, Office of Research and Development, Biomedical Laboratory and Development CDA-2 Award 005-10S (to E.S.); Department of Veterans Affairs Merit Review Award I01-BX002949 (to E.S.); Department of Defense Congressionally Directed Medical Research Program Award W81XWH-18-1-0598 (to E.S.); National Institutes of Health (NIH) Grant F31-NS098597 (to W.D.H.); NIH Grant R01-NS080979 (to G.L.W.); and NIH Grant P30-NS061800 (OHSU Advanced Light Microscopy Core). The contents of this manuscript do not represent the views of the US Department of Veterans Affairs or the US government.

1. Nicoll RA, Schmitz D (2005) Synaptic plasticity at hippocampal mossy fibre synapses. *Nat Rev Neurosci* 6:863–876.
2. Vyleta NP, Borges-Merjane C, Jonas P (2016) Plasticity-dependent, full detonation at hippocampal mossy fiber-CA3 pyramidal neuron synapses. *eLife* 5:e17977.
3. Sutula T, He XX, Cavazos J, Scott G (1988) Synaptic reorganization in the hippocampus induced by abnormal functional activity. *Science* 239:1147–1150.
4. Sutula T, Cascino G, Cavazos J, Parada I, Ramirez L (1989) Mossy fiber synaptic reorganization in the epileptic human temporal lobe. *Ann Neurol* 26:321–330.
5. Houser CR, et al. (1990) Altered patterns of dynorphin immunoreactivity suggest mossy fiber reorganization in human hippocampal epilepsy. *J Neurosci* 10:267–282.
6. Okazaki MM, Evenson DA, Nadler JV (1995) Hippocampal mossy fiber sprouting and synapse formation after status epilepticus in rats: Visualization after retrograde transport of biocytin. *J Comp Neurol* 352:515–534.

7. Cavazos JE, Zhang P, Qazi R, Sutula TP (2003) Ultrastructural features of sprouted mossy fiber synapses in kindled and kainic acid-treated rats. *J Comp Neurol* 458:272–292.
8. Hendricks WD, Chen Y, Bensen AL, Westbrook GL, Schnell E (2017) Short-term depression of sprouted mossy fiber synapses from adult-born granule cells. *J Neurosci* 37:5722–5735.
9. Sutula T, et al. (1998) Synaptic and axonal remodeling of mossy fibers in the hilus and supragranular region of the dentate gyrus in kainate-treated rats. *J Comp Neurol* 390:578–594.
10. Smith BN (2017) Sprouted mossy fiber connections of adult-born granule cells: Detonate or fizzle? *Epilepsy Curr* 17:379–380.
11. Buckmaster PS (2014) *Does Mossy Fiber Sprouting Give Rise to the Epileptic State? Issues in Clinical Epileptology: A View from the Bench*, eds Scharfman HE, Buckmaster PS (Springer Netherlands, Dordrecht, The Netherlands), Vol 813, pp 161–168.
12. Longo BM, Mello LEAM (1997) Blockade of pilocarpine- or kainate-induced mossy fiber sprouting by cycloheximide does not prevent subsequent epileptogenesis in rats. *Neurosci Lett* 226:163–166.
13. Longo BM, Mello LEAM (1998) Supragranular mossy fiber sprouting is not necessary for spontaneous seizures in the intrahippocampal kainate model of epilepsy in the rat. *Epilepsy Res* 32:172–182.
14. Mello LE, et al. (1993) Circuit mechanisms of seizures in the pilocarpine model of chronic epilepsy: Cell loss and mossy fiber sprouting. *Epilepsia* 34:985–995.
15. Scharfman HE, Sollas AL, Berger RE, Goodman JH (2003) Electrophysiological evidence of monosynaptic excitatory transmission between granule cells after seizure-induced mossy fiber sprouting. *J Neurophysiol* 90:2536–2547.
16. Cronin J, Obenaus A, Houser CR, Dudek FE (1992) Electrophysiology of dentate granule cells after kainate-induced synaptic reorganization of the mossy fibers. *Brain Res* 573:305–310.
17. Wuarin JP, Dudek FE (2001) Excitatory synaptic input to granule cells increases with time after kainate treatment. *J Neurophysiol* 85:1067–1077.
18. Cheng X, et al. (2011) Pulse labeling and long-term tracing of newborn neurons in the adult subgranular zone. *Cell Res* 21:338–349.
19. Rosenmund C, Clements JD, Westbrook GL (1993) Nonuniform probability of glutamate release at a hippocampal synapse. *Science* 262:754–757.
20. Moore KA, Nicoll RA, Schmitz D (2003) Adenosine gates synaptic plasticity at hippocampal mossy fiber synapses. *Proc Natl Acad Sci USA* 100:14397–14402.
21. Fedele DE, et al. (2005) Astrogliosis in epilepsy leads to overexpression of adenosine kinase, resulting in seizure aggravation. *Brain* 128:2383–2395.
22. Boison D (2008) The adenosine kinase hypothesis of epileptogenesis. *Prog Neurobiol* 84:249–262.
23. Sandau US, et al. (2016) Adenosine kinase deficiency in the brain results in maladaptive synaptic plasticity. *J Neurosci* 36:12117–12128.
24. Williams-Karnesky RL, et al. (2013) Epigenetic changes induced by adenosine augmentation therapy prevent epileptogenesis. *J Clin Invest* 123:3552–3563.
25. Buckmaster PS (2012) Mossy fiber sprouting in the dentate gyrus. *Jasper's Basic Mechanisms of the Epilepsies*, eds Noebels JL, Avoli M, Rogawski MA, Olsen RW, Delgado-Escueta AV (Natl Center Biotechnol Inf, Bethesda), p 29.
26. Sutula TP, Dudek FE (2007) Unmasking recurrent excitation generated by mossy fiber sprouting in the epileptic dentate gyrus: An emergent property of a complex system. *Prog Brain Res* 163:541–563.
27. Hardison JL, Okazaki MM, Nadler JV (2000) Modest increase in extracellular potassium unmasks effect of recurrent mossy fiber growth. *J Neurophysiol* 84:2380–2389.
28. Patrylo PR, Dudek FE (1998) Physiological unmasking of new glutamatergic pathways in the dentate gyrus of hippocampal slices from kainate-induced epileptic rats. *J Neurophysiol* 79:418–429.
29. Wuarin JP, Dudek FE (1996) Electrographic seizures and new recurrent excitatory circuits in the dentate gyrus of hippocampal slices from kainate-treated epileptic rats. *J Neurosci* 16:4438–4448.
30. Santhakumar V, Aradi I, Soltesz I (2005) Role of mossy fiber sprouting and mossy cell loss in hyperexcitability: A network model of the dentate gyrus incorporating cell types and axonal topography. *J Neurophysiol* 93:437–453.
31. Amorim BO, et al. (2016) Effects of A1 receptor agonist/antagonist on spontaneous seizures in pilocarpine-induced epileptic rats. *Epilepsy Behav* 61:168–173.
32. Gouder N, Fritschy JM, Boison D (2003) Seizure suppression by adenosine A1 receptor activation in a mouse model of pharmacoresistant epilepsy. *Epilepsia* 44:877–885.
33. Tauck DL, Nadler JV (1985) Evidence of functional mossy fiber sprouting in hippocampal formation of kainic acid-treated rats. *J Neurosci* 5:1016–1022.
34. von Kitzing E, Jonas P, Sakmann B (1994) Quantal analysis of excitatory postsynaptic currents at the hippocampal mossy fiber-CA3 pyramidal cell synapse. *Adv Second Messenger Phosphoprotein Res* 29:235–260.
35. Ben-Simon Y, et al. (2015) A combined optogenetic-knockdown strategy reveals a major role of tomosyn in mossy fiber synaptic plasticity. *Cell Rep* 12:396–404.
36. Jackman SL, Turecek J, Belinsky JE, Regehr WG (2016) The calcium sensor synaptotagmin 7 is required for synaptic facilitation. *Nature* 529:88–91.
37. Toth K, Suares G, Lawrence JJ, Philips-Tansey E, McBain CJ (2000) Differential mechanisms of transmission at three types of mossy fiber synapse. *J Neurosci* 20:8279–8289.
38. Zhou QG, et al. (2019) Chemogenetic silencing of hippocampal neurons suppresses epileptic neural circuits. *J Clin Invest* 129:310–323.
39. Shibley H, Smith BN (2002) Pilocarpine-induced status epilepticus results in mossy fiber sprouting and spontaneous seizures in C57BL/6 and CD-1 mice. *Epilepsy Res* 49:109–120.